IOWA STATE UNIVERSITY
Digital Repository

Retrospective Theses and Dissertations

Iowa State University Capstones, Theses and Dissertations

1965

A model of terrestrial radio wave propagation using a laser

Mark Roman Guidry Jr.
Iowa State University

Follow this and additional works at: https://lib.dr.iastate.edu/rtd

Part of the Electrical and Electronics Commons

Recommended Citation
Guidry, Mark Roman Jr., "A model of terrestrial radio wave propagation using a laser " (1965). *Retrospective Theses and Dissertations*. 4007.
https://lib.dr.iastate.edu/rtd/4007

This Dissertation is brought to you for free and open access by the Iowa State University Capstones, Theses and Dissertations at Iowa State University Digital Repository. It has been accepted for inclusion in Retrospective Theses and Dissertations by an authorized administrator of Iowa State University Digital Repository. For more information, please contact digirep@iastate.edu.

المنارة للاستشارات

www.manaraa.com

This dissertation has been microfilmed exactly as received 65-7613

GUIDRY, Jr., Mark Roman, 1937-
A MODEL OF TERRESTRIAL RADIO WAVE PROPAGATION USING A LASER.

Iowa State University of Science and Technology
Ph.D., 1965
Engineering, electrical

University Microfilms, Inc., Ann Arbor, Michigan

A MODEL OF TERRESTRIAL RADIO WAVE PROPAGATION USING A LASER

by

Mark Roman Guidry, Jr.

A Dissertation Submitted to the
Graduate Faculty in Partial Fulfillment of
The Requirements for the Degree of
DOCTOR OF PHILOSOPHY

Major Subject: Electrical Engineering

Approved:

Signature was redacted for privacy.

In Charge of Major Work

Signature was redacted for privacy.

Head of Major Department

Signature was redacted for privacy.

Dean of Graduate College

Iowa State University
Of Science and Technology
Ames, Iowa

1965

PLEASE NOTE:
Figure pages are not original copy. They tend to "curl". Filmed in the best possible way.
University Microfilms, Inc.

TABLE OF CONTENTS

		Page
I.	INTRODUCTION	1
II.	THEORY	8
III.	EXPERIMENTAL SET-UP	24
	A. Source of Electromagnetic Waves	24
	B. Analog Model of Terrestrial Surface	37
	C. Detector of Electromagnetic Energy	46
IV.	ANALYSIS OF RESULTS	63
V.	CONCLUSIONS	76
VI.	LITERATURE CITED	79
VII.	ACKNOWLEDGMENTS	83

I. INTRODUCTION

This is the report of an experimental model study conducted to obtain the variation in intensity of electromagnetic energy as it propagates beyond the radio horizon of a terrestrial surface. The experimental set-up, as diagrammed in Figure 1, consisted of an aperture illuminated by a gas laser as a source, a pyrex disc constructed as a scale model of the terrestrial surface, and a photographic detector. At points beyond the radio horizon, range and altitude variations of field intensity have been obtained and compared with classical diffraction theory.

The study of electromagnetic propagation around spherical bodies has been of interest since the earliest days of radio. The range of communication via radio is determined by the rate at which electromagnetic energy is attenuated as it propagates over the earth's spherical surface. The first attempts to answer this question of range attenuation were applications of earlier results of Lord Rayleigh (30). His solution took the form of an infinite series of spherical harmonics. While the series converges rapidly for small particles, it is practically useless in cases where the diameter of the sphere is large compared to the wavelength. For the earth's radius, at radio frequencies hundreds of terms are necessary for reasonable accuracy.

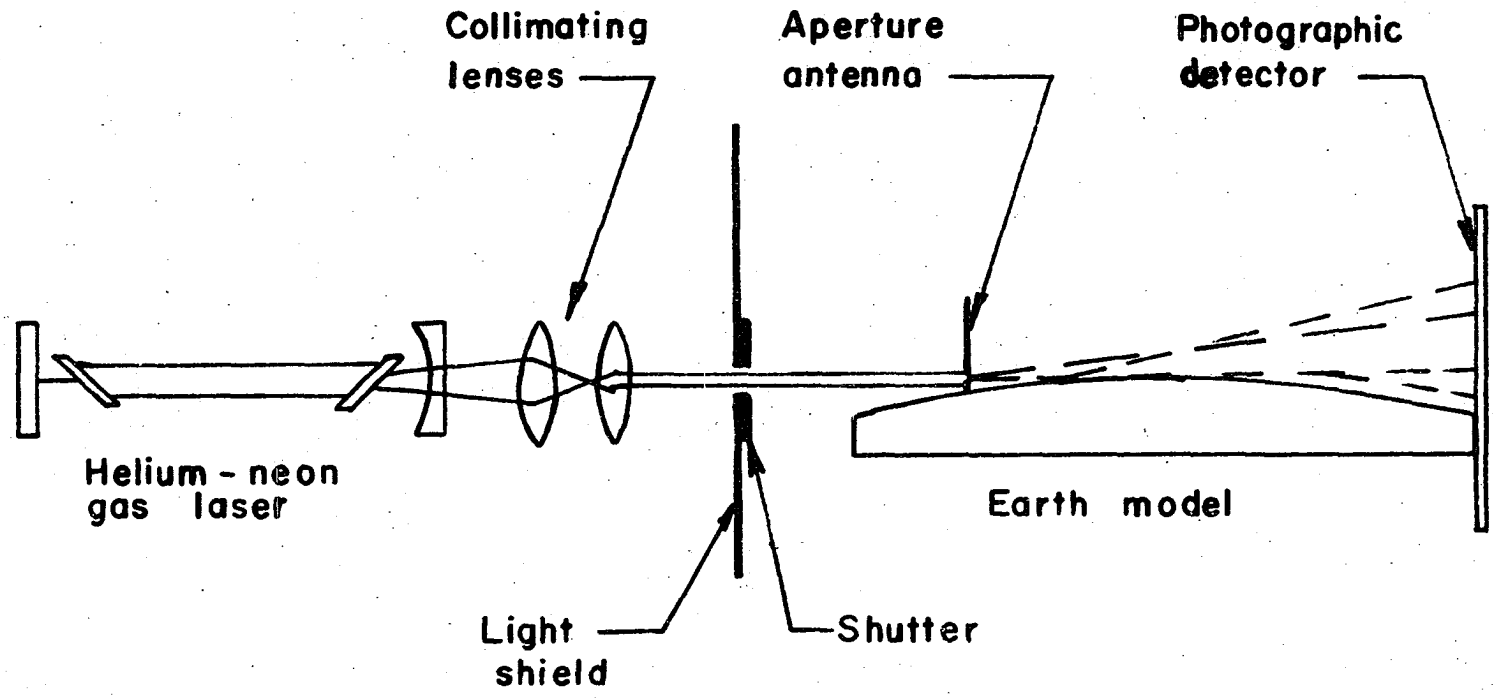

Figure 1. Diagram of experimental set-up

The early 1900's saw numerous attempts to obtain more useful results, all of which were criticized by later workers for their non-rigorous approach. The analysis was finally put on a sound footing by Watson (38) in 1919. Watson developed a transformation which changed Rayleigh's infinite series into a contour integral. The integral is then evaluated by the method of residues. This analysis was limited to fields at the surface of the sphere and only those due to vertical polarization. In 1933, Schelleng, Burrows, and Ferrell (31) proposed a model in which atmospheric refraction could be taken into account by using a homogeneous atmosphere and an earth with an effective radius equal to 4/3 the actual radius. van der Pol and Bremmer (36), in 1938, extended Watson's analysis to include arbitrary conductivity of the earth and an arbitrary dielectric constant. Their solution placed special emphasis on approximations of practical value, and the results were well suited for numerical computations. These results, coupled with the earth-flattening approximation to account for atmospheric refraction, were generally accepted and frequently used. It was felt that the problem had been solved.

During the war years, higher power outputs and larger antennas were developed at higher frequencies. First indications of trouble to come were reports of radar ranges much greater than expected. The concept of an atmospheric duct was introduced to explain the differences. However,

as more data were made available, it became clear that long distance transmission occurred more frequently than the meterological conditions required by the duct theory. Propagation was found to be consistently much greater than expected. An indication of the seriousness of the problem as pointed out by Carroll and Ring (8) and Bullington (6), was the interference due to the overlapping of television station transmissions. It was found necessary to "freeze" construction of new television stations until better estimates of range could be obtained. Reliable experimental field strength measurements were published by Megaw (24) and Gerks (14). These measurements indicated that fields beyond the radio horizon were always stronger than predicted by as much as 60 db. This stimulated a more critical study of the entire problem. There emerged two separate hypotheses to explain the differences.

The "turbulent scatterer" theory was advanced by Booker and Gordon (3), who argued that local, time varying anomalies in the refractive index, called "blobs", effectively scatter energy beyond the horizon. This theory is particularly successful in explaining the statistical variation in the received signal. The main criticism (34) is that there are numerous adjustable parameters which allow one to fit the theory to the results without recourse to experimental verification of these parameters. To the present day, experiments are continuing in an attempt to correlate

meteorological data with the predictions of this theory. Some have been shown to support the hypothesis and others do not (1).

A second group of investigators made a more critical study of the original mode theory in an attempt to bring together experimental and theoretical results. Pryce (29) rederived the classical results in a more straight forward manner. His results are in the form of a series which is highly convergent for fields beyond the horizon. Since his results are quite general and meet all conditions of this experiment, they will be used to compare with the experimentally measured values. A more detailed discussion of his work is included in Chapter II.

Bullington (5) considered the effects of surface roughness. Wait (37) carefully analyzed the assumption of a homogeneous earth and concluded that such a model was justified. Carroll (7) and Carroll and Ring (8) showed that for several approximations to the actual atmospheric refractive index profiles, higher order modes could make a significant contribution. More recently, Budden (4) has reviewed the standard mode theory and generalized it to include effects of the ionosphere. His results are of the same form, namely Airy integral solutions, as Pryce (29) but extended to more general profiles of refractive index and ionosphere effects. Gerks (13) has reviewed the entire mode solution as it applies to a spherical earth and a

stratified profile. All of these methods are criticized for their inability to include time varying factors to account for the statistical fluctuations of the received signal. Some other extensions of the normal mode theory for more general profiles and to bring it into agreement with measurements have been made by Post (27) and Johnson (20). At present, the two basic hypotheses to explain the large fields existing beyond the horizon are considered with insufficient evidence to justify one or the other.

The reason for this is that experiments carried out under actual conditions existing on the earth contain numerous parameters which are varying in time. For example, to measure range variations in field intensity requires an array of identical antennas or an antenna that can be transported in range. The attempts to transport antennas in range have resulted in data obviously affected by atmospheric changes. It is also impossible to measure all of the parameters needed, such as the profile of the refractive index.

Problems of this type are ideally suited to model studies. The use of a model permits the numerous factors to be well determined and controlled. Models are well accepted tools for use in radio propagation studies. Skolnik (33) has scaled antenna arrays to study the effects of non-uniform or pseudo-random element spacings. Furutsu (12)

and Maley and Ottesen (22) have gone to higher frequencies to scale electromagnetic propagation over the earth in observing the effects of mixed paths. Edison (10) and Tolopko (35) report on work using acoustic waves in water with induced turbulence to study the effects of turbulent scatter. A limitation in using microwaves or acoustical waves as sources in models is the inability to generate wavelengths significantly shorter than one centimeter. This limits the scale factor to something less than 10^4:1. As a result, the path lengths are limited to cases where the earth's surface is assumed flat. With the use of a gas laser as a source, the scale factor can be increased to values greater than 10^6:1. Huntley (15, 16, 17) suggests using a laser as a model source and obtains qualitative results for an antenna array. He suggests that since the scale factor is so large, this would be a useful tool in studying diffraction due to mountainous terrain.

II. THEORY

The problem under consideration is that of electromagnetic wave propagation over a spherical surface where the radius of the sphere is large compared to a wavelength. In particular, the problem is restricted to the case of a perfectly smooth surface imbedded in a homogeneous medium. As mentioned in the Introduction, the method of Pryce (29) constitutes a theoretical formulation quite applicable to the case under consideration. His results are in a convenient form and sufficiently general to include all factors which are present in the experimental results.

The method used by Pryce is known as the earth-flattening model. It is called this because Pryce applies a coordinate transformation to Maxwell's equations to obtain a set of approximate differential equations. The transformation effectively flattens a small portion of the sphere around the source. It simultaneously yields curved ray paths from previously straight ones to retain the relative curvature between the ray and surface, the essential feature of the problem. In essence, the method is approximately equivalent to treating the earth's surface as "flat" and space as curved.

The advantage of this model is that approximations are made in the differential equations and the resulting simplified equations are solved. Subsequent approximations are

more straight forward. From the mathematical standpoint this method is easier because the slowly convergent series in Legendre polynominals or Hankel functions of the classical papers of Watson (38) and van der Pol and Bremmer (36) are replaced by Airy integrals. The essential simplification is that instead of transforming and approximating by various techniques the solution of the exact differential equations, one first approximates the differential equation. The gain in simplicity, unfortunately, is offset by a loss in rigor. This loss in rigor occurs because it is more difficult to estimate the error made in using the approximate differential equation. Pryce has made no attempt to justify the method rigorously; however, a partial investigation of this has been made by Pekaris (26). A summary of Pryce's results will be presented below. For a detailed derivation of these results see reference (29).

The coordinates to be used are denoted by x, y, z. They are defined in terms of spherical polar coordinates R, θ, φ whose origin is at the center of the sphere and whose polar axis passes through the source as shown in Figure 2. The defining equations are

$$\begin{aligned} x &= a\,\theta \cos\varphi \\ y &= a\,\theta \sin\varphi \\ z &= a \log(R/a), \end{aligned} \tag{1}$$

where a is the radius of the spherical surface. x, y, z

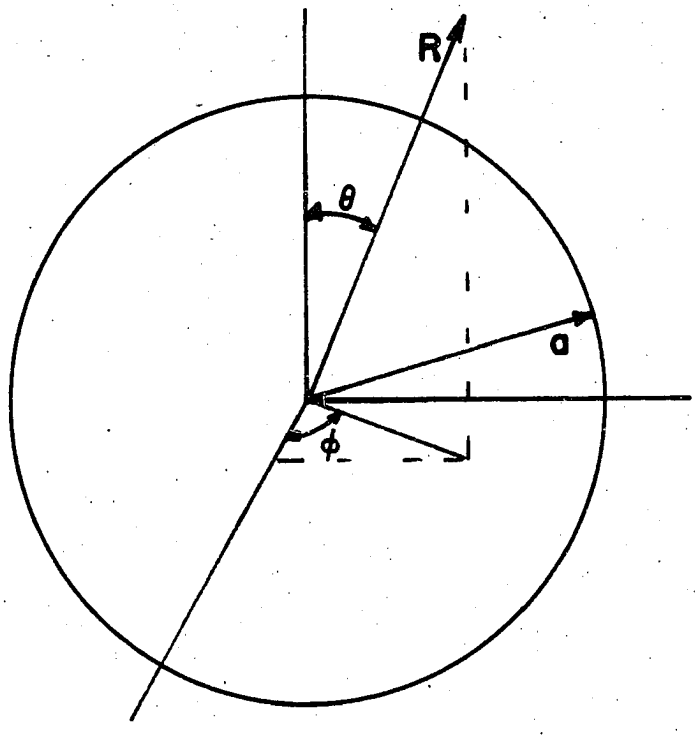

Figure 2. The spherical polar coordinates of the problem

are approximately rectangular Cartesian coordinates in the neighborhood of the source of radiation. Originally Pryce used the more conventional transformation given by:

$$\begin{aligned} x &= a \sin\theta \cos\varphi \\ y &= a \sin\theta \sin\varphi \\ z &= R-a \end{aligned} \qquad (2)$$

He states that the present formulation, as given by Equation 1, offers considerable formal simplification. Note that now

$$r = \sqrt{x^2 + y^2} = a\theta$$

becomes the horizontal distance along the spherical surface measured from the pole. Also, when $\ln(R/a)$ is expanded in a power series one obtains

$$z = a \ln(R/a) = a\left[(R/a - 1) - 1/2(R/a - 1)^2 + \ldots\right] \qquad (3)$$

For $R/a \approx 1$, z is approximated by $z \approx R - a$, the radial distance from the spherical surface. The surface of the sphere is characterized by $z = 0$.

When this coordinate transformation is applied to Maxwell's equations, there result terms in powers of $1/a$. Pryce's method at this point neglects all terms in $(1/a)^2$ and higher powers of $1/a$ occurring in Maxwell's transformed

equations while retaining those in $1/a$. It turns out that the resulting equations are invariant under translations of x and y allowing the problem to be solved by application of Fourier transforms.

All quantities are assumed to vary sinusoidally at a single frequency ω and thus contain a factor $\exp(i\omega t)$. This term will not be included in the equations and it is understood that to obtain the actual fields one must insert it and take the real part of the resulting expression. The field vectors $\vec{E}$, $\vec{H}$ can be expressed in terms of their Fourier transforms with respect to x and y giving:

$$\vec{E}(x,y,z) = \iint \tilde{E}(\alpha,\beta,z)e^{i(\alpha x+\beta y)}d\alpha d\beta$$

$$\vec{H}(x,y,z) = \iint \tilde{H}(\alpha,\beta,z)e^{i(\alpha x+\beta y)}d\alpha d\beta \qquad (4)$$

These transformed quantities $\tilde{E}$, $\tilde{H}$ are inserted into Maxwell's equations, appropriate for the coordinate system, with all terms $(1/a)^2$ and higher powers in $1/a$ omitted. Fourier transforms of the appropriate source functions also appear in the equations. By the usual techniques, these equations can be reduced to four second order equations. Two of these equations determine $\tilde{E}$. One determines $\tilde{E}$ inside the sphere; the other, $\tilde{E}$ outside. Similarly $\tilde{H}$ is determined. The equations are:

$$\left[\frac{d^2}{dz^2} + \mathcal{K}^2 - \alpha^2 - \beta^2 + \frac{2\mathcal{K}^2}{a} z\right] \tilde{E} \equiv \tilde{S}_1$$

$$\left[\frac{d^2}{dz^2} + \mathcal{K}^2 - \alpha^2 - \beta^2 + \frac{2\mathcal{K}^2}{a} z\right] \tilde{H} \equiv \tilde{S}_2 \qquad (5)$$

for outside the sphere; and

$$\left[\frac{d^2}{dz^2} + \epsilon' \mathcal{K}^2 - \alpha^2 - \beta^2 + \frac{2\epsilon'\mathcal{K}^2}{a} z\right] \tilde{E} \equiv 0$$

$$\left[\frac{d^2}{dz^2} + \epsilon' \mathcal{K}^2 - \alpha^2 - \beta^2 + \frac{2\epsilon'\mathcal{K}^2}{a} z\right] \tilde{H} \equiv 0 \qquad (6)$$

for inside the sphere. Here α, β are variables conjugate to x, y in Fourier space, $\mathcal{K} = \frac{2\pi}{\lambda}$ is the wave number, ϵ' is the complex dielectric constant of the earth, and $\tilde{S}_1$, $\tilde{S}_2$ are Fourier transforms of the source functions. The complex dielectric constant of the earth is given by:

$$\epsilon' = \epsilon_e - \frac{i\ 18{,}000\ \sigma}{f_{mc}} \qquad (7)$$

where ϵ_e is the relative dielectric constant of the earth and σ is the conductivity of the earth.

An important assumption used to arrive at this point is that the variation in dielectric constant external to the sphere takes place only in the z direction and that this

variation with z takes place in an approximately linear fashion in the region of importance. As mentioned in the Introduction, Schelleng, Burrows, and Ferrell (31) have shown that propagation in a stratified medium, where the variation is approximately a linear decrease, is equivalent to propagation in free space above a sphere of modified radius a'.

Budden (4) states that the refractive index η of moist air is given approximately by:

$$\eta = \sqrt{\epsilon\mu} = 1 + (79\,\frac{p}{T} - 10\,\frac{e}{T} + 3.8\,\frac{e}{T^2}\,x10^5)\;10^{-9} \qquad (8)$$

where p is the total atmospheric pressure (dynes/cm^2), e is the partial pressure of water vapor, and T is the absolute temperature. For variations limited to low values of z the effects of p and e dominate the effects of T and the result under normal turbulent conditions is that:

$$-\frac{d\eta}{dz} = k \approx 4 \times 10^{-5}/\text{km} \qquad (9)$$

where k is called the "lapse rate of refractive index." The value 4×10^{-5}/km is typical of normal conditions that give rise to a so-called standard atmosphere. Budden also shows that

$$\frac{1}{a'} = \frac{1}{a} - k \qquad (10)$$

thus, under so-called standard conditions the actual earth's radius of 6.36×10^6m is replaced by a modified radius a' where $a' \approx 4/3\ a$.

On occasions, particularly in tropical climates where water vapor content changes by large amounts in relatively small altitude changes, the lapse rate may be large enough to cause the effective earth radius to be negative. In this case the propagation is called "anomalous propagation" or ducting. For anomalous propagation Pryce's model breaks down completely and it is necessary to use methods such as Budden's, which treat this problem in terms of guided waves. It is possible for the variation in refractive index to be normal at the earth's surface but abnormal at higher elevations resulting in what is known as elevated ducts. In any case, Pryce's analysis is strictly limited to the case of normal propagation ($\infty > a' > 0$) and because of the equivalence it is assumed that $\epsilon = \mu = 1$ outside the sphere.

Inside the sphere, the region near the surface is assumed homogeneous with $\mu = 1$ and ϵ' as given in Equation 7. The conductivity is necessary to insure that the waves entering the sphere are damped. This guarantees that internal reflections do not result in energy returning to the surface. Thus, when boundary conditions are considered, the fields inside the sphere are only waves travelling

inward. No waves travelling toward the surface from the interior are considered. It is also assumed that the interior of the sphere contains no sources.

In order to solve Equations 5 and 6, they can, by a change of variable, be shown to be directly related to the differential equation:

$$\frac{d^2}{d\xi^2} u(\xi) = \xi u(\xi) \tag{11}$$

This equation has as its solution the Airy integral functions $Ai(\xi)$ and $Bi(\xi)$. The solution can also be expressed in terms of Hankel functions of order 1/3 but the properties of the Airy integrals are considerably simpler to work with when constructing a solution to match the boundary conditions.

It is interesting to note that the terms in z in the differential operators in Equation 5 and 6 came from the approximation

$$e^{\frac{2z}{a}} \approx 1 + \frac{2z}{a} \tag{12}$$

If this approximation is not made the equations are solvable in terms of Bessel functions of argument $\varkappa a e^{z/a}$. But this would entail the use of asymptotic forms of Bessel functions of arbitrary order for large values of argument. Asymptotic forms of Bessel functions of arbitrary order for

large arguments in turn rest on the theory of the Airy integral, which is a fundamentally simpler function.

Thus, the solutions to Equations 5 and 6 are expressed in terms of Airy integrals. These solutions are chosen so as to satisfy the boundary condition at the surface of the sphere and the condition of outward propagation of energy at large z. The inverse Fourier transform now leads to a solution in the form of a definite integral. This complex integral can be approximated by an infinite integral which is then reduced to a contour integral. The contour integral can be evaluated by the method of residues. The solution thus takes the form of an infinite sum of these residues. Its great value lies in the fact that it converges quite rapidly for fields beyond the horizon. For many practical applications of propagation beyond the horizon the series can be approximated by a single term.

As a check on the validity of the earth-flattening transformation, it is possible to evaluate the infinite integrals by the saddle point method and obtain an approximate value for the integrals applicable to line of sight propagation. Ray or geometrical optics furnish good verification of these results.

The results of Pryce's method indicate that the field strength produced over a smooth, spherical earth, expressed in terms of the free-space field strength is given by:

$$\frac{|\mathcal{E}|}{|\mathcal{E}_{fs}|} = \sqrt{r\lambda} \left| \sum_{s=1}^{\infty} G_s(h/h_o)\, G_s(\tfrac{z}{h_o})\, F_s\,(r/d_o) \right| /h_o \quad (13)$$

where r = distance between antennas

h = height of transmitting antenna

z = height of receiving antenna

The terms h_o and d_o are called the scale height and scale distance respectively and are given by:

$$h_o = 1/2\ (a'\ \lambda^2/\pi^2)^{1/3} \quad (14)$$

and

$$d_o = (a'^2\ \lambda/\pi)^{1/3} \quad (15)$$

where a' is the effective or modified earth's radius. The function $F_s(r/d_o)$ is given by:

$$F_s(r/d_o) = \exp i(a_s\ r/d_o) \quad (16)$$

where a_s is a solution of the equation

$$f\ (a_s) = T\ f'(a_s) \quad (17)$$

where T is a number dependent on the polarization of the field and the properties of the surface. The function $f(a_s)$ can be expressed in terms of the Airy integral

$$f(a_s) = 2e^{-i\ \pi/6}\ \ Ai(a_s\ e^{i\ \pi/3}) \quad (18)$$

The function $G_s(h/h_o)$ and $G_s(z/h_o)$ are called the height-gain functions since they determine the effect antenna height has on measured field strength. They are defined as:

$$G_s(h/h_o) = \frac{f(a_s+h/h_o)}{(1+T^2a_s)^{1/2}f'(a_s)} \tag{19}$$

Any polarized field can be considered to be the linear combination of two independent fields, one polarized in the horizontal plane and the other polarized in the vertical plane. Since the reflection at the surface is different for different polarizations, the results would be expected to be dependent upon polarization. Pryce's results have the polarization dependence of the fields completely contained in the value of T. It is through the parameter T that the solution is made to satisfy the boundary conditions at the surface. T is given by:

$$T_1 = -i\,\frac{\epsilon'}{K(\epsilon'-1)^{1/2}} \tag{20}$$

for vertical polarization, and

$$T_2 = -i\,\frac{1}{K(\epsilon'-1)^{1/2}} \tag{21}$$

for horizontal polarization, where

$$K = 2\pi h_o/\lambda = (\pi\ a/\lambda)^{1/3} \tag{22}$$

and ϵ' is given by Equation 7. The variation of T_1 and T_2 with frequency for several types of surfaces as given by Gerks (13) is shown in Figures 3, 4 and 5. Generally the value of T is small enough to justify setting it equal to zero. This is almost always true for horizontal polarization. When T is zero several simplifications result. Equation 17 becomes

$$f(a_s) = 0 \tag{23}$$

The magnitudes of a_s now are simply the zeros of the Airy integral and the argument for all a_s is $2\pi/3$. The height-gain function $G_s(h/h_o)$ becomes:

$$G_s(h/h_o) = \frac{f(a_s+h/h_o)}{f'(h/h_o)} \tag{24}$$

The zeros of the Airy integral are well known and the first five are given in Table 1. The function $G_s(h/h_o)$ as given in Equation 24 has been tabulated by Domb (9) for the first five roots.

Table 1. Zeros of the Airy integral

S	1	2	3	4	5
$\lvert a_s \rvert$	2.3381	4.0879	5.5206	6.7867	7.9441

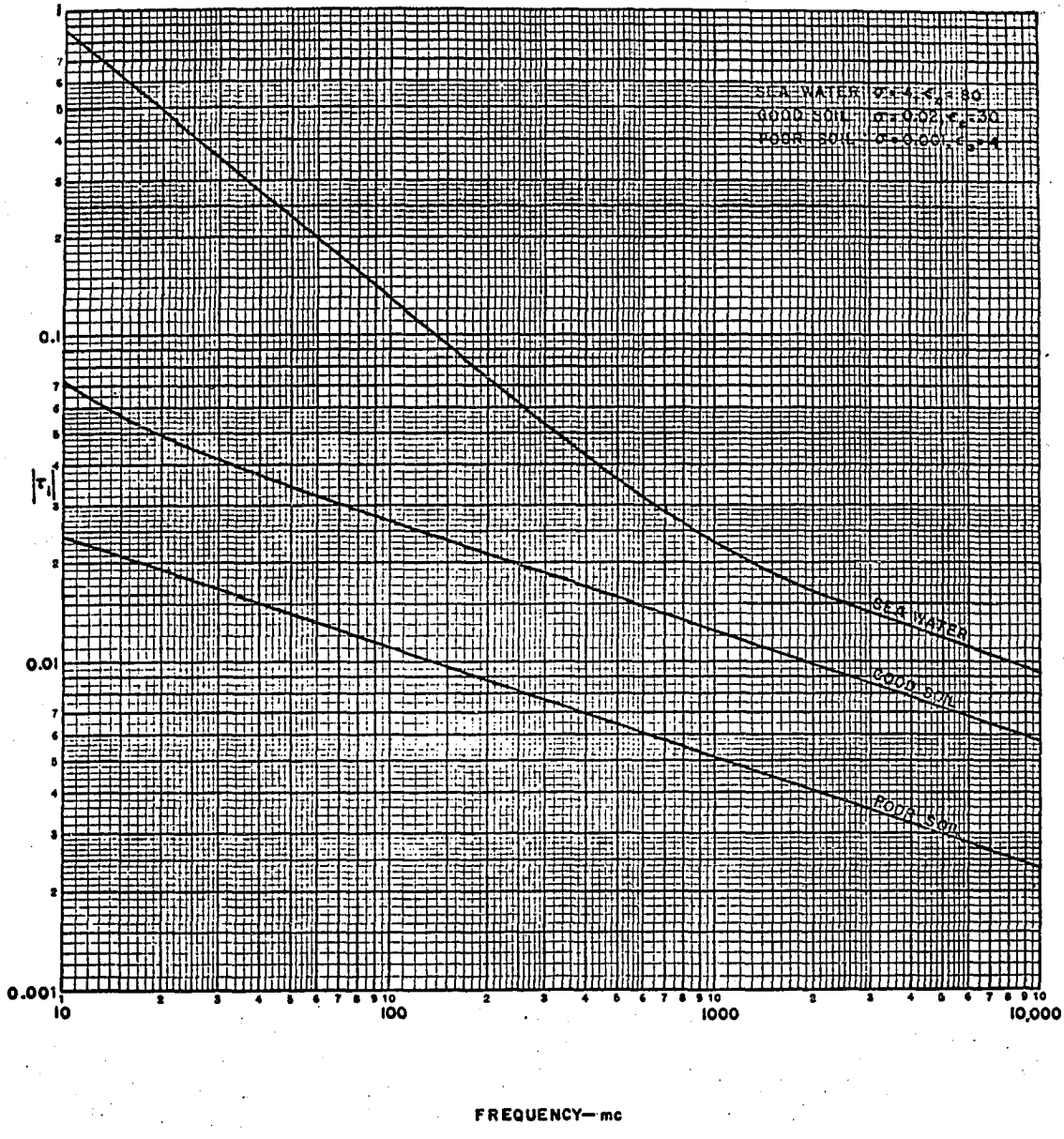

Figure 3. Magnitude of τ_1 versus frequency (after Gerks (13))

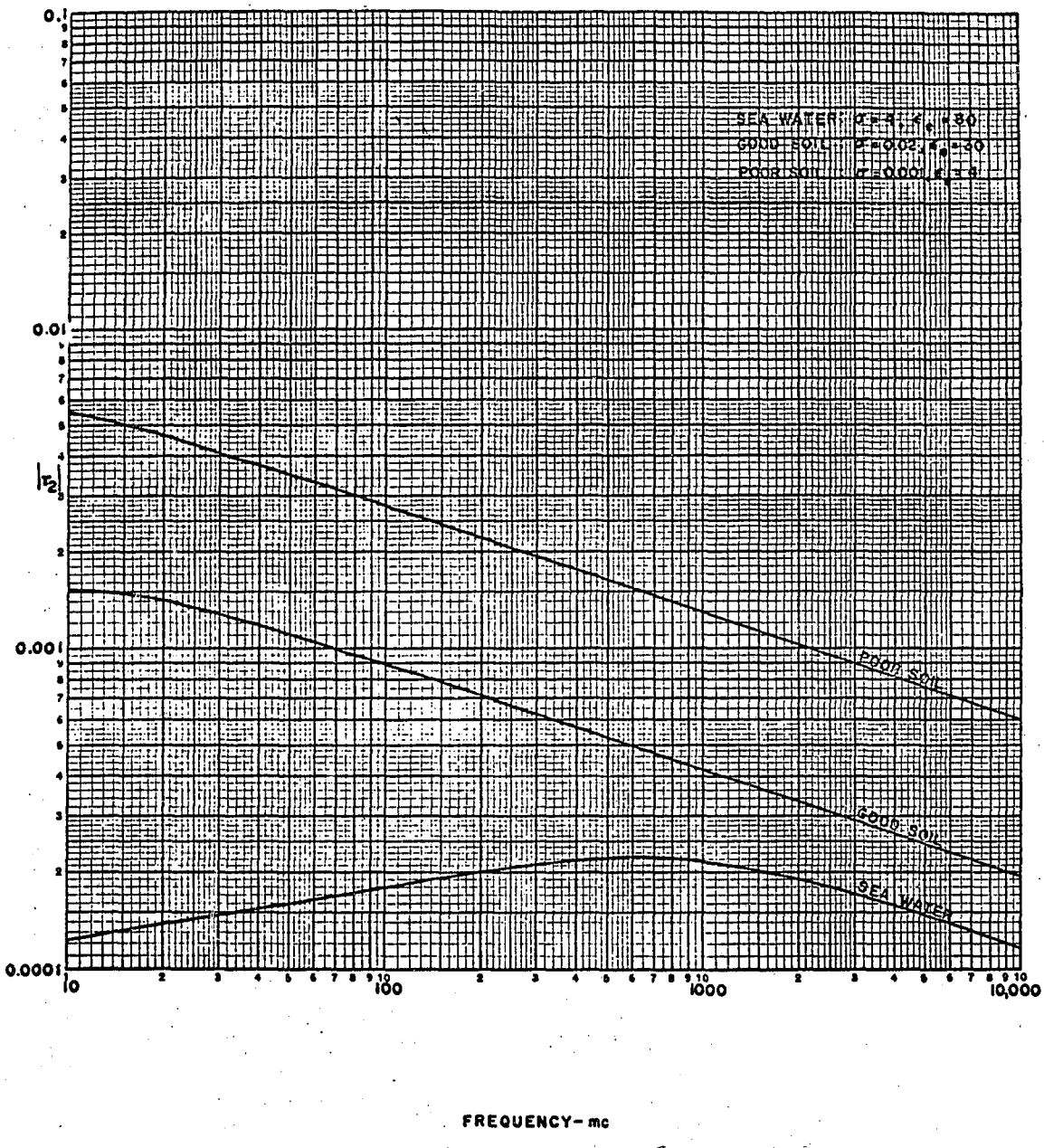

Figure 4. Magnitude of τ_2 versus frequency
(after Gerks (13))

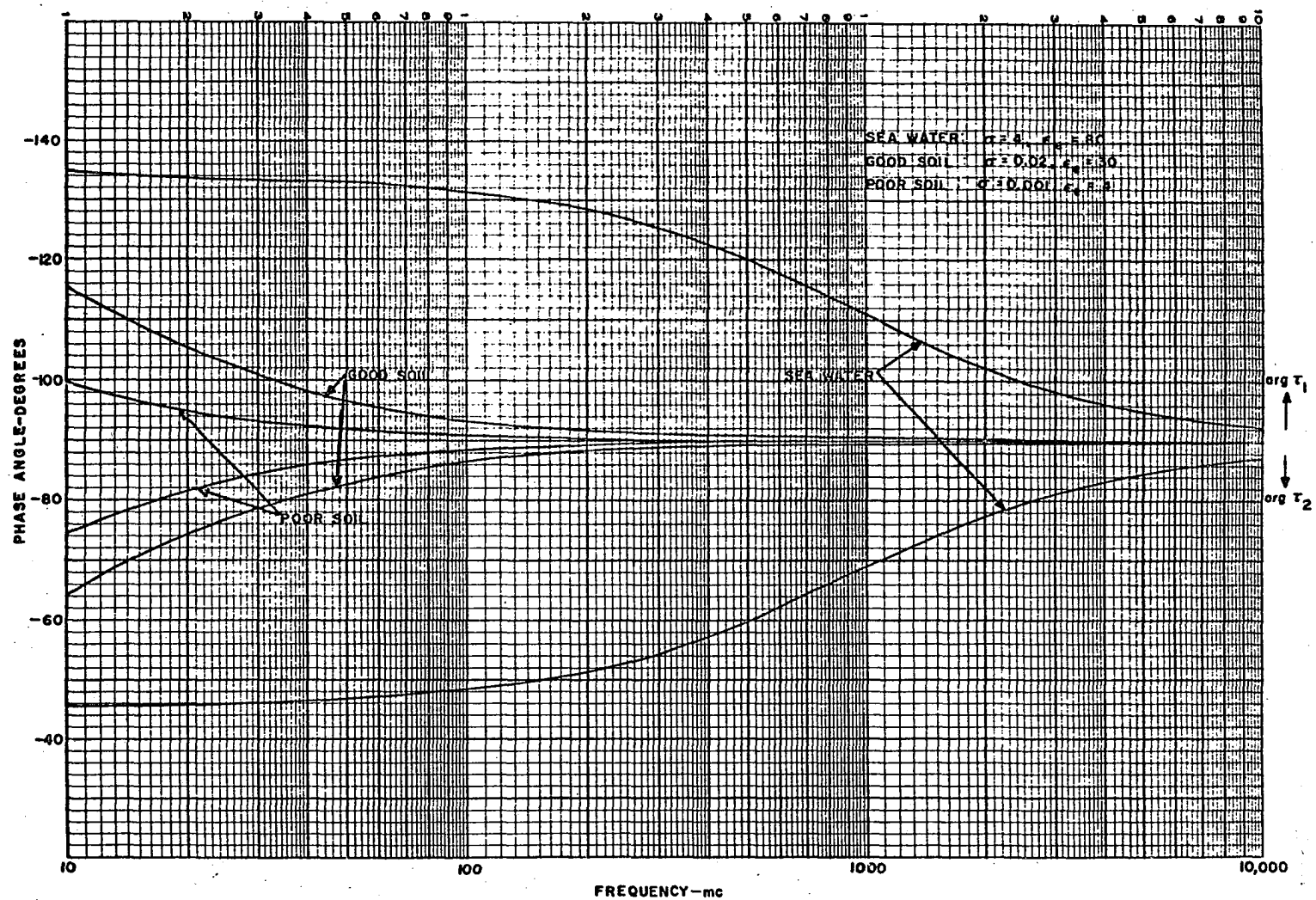

Figure 5. Argument of τ_1 and τ_2 versus frequency (after Gerks (13))

III. EXPERIMENTAL SET-UP

A. Source of Electromagnetic Waves

The source used in this experiment was a circular aperture illuminated by a helium-neon gas laser. The laser produces a stable continuous output at 6328 Å which is visible as an intense deep red color. Discharge excitation was furnished by a radio frequency transmitter. The transmitter furnished about 75 watts at 27.2 megacycles for normal operation. The discharge tube itself is quartz with Brewster angle windows at each end allowing the use of external mirrors. Forming the ends of the optical cavity were two dielectric mirrors. These mirrors reflect more than 99 percent of the light incident upon them in a range of from 5500 Å to 6700 Å. Transmission in this range is less than 1/2 percent. Plastic dust shields cover the region between the ends of the discharge tube and the mirrors. Dust in this region is capable of scattering large amounts of light out of the cavity and thus causing large fluctuations in laser output.

Skolnik (33) has pointed out that when a plane wave is incident on one side of a test aperture the radiation pattern of energy that emerges from the other side is essentially the same as the radiation pattern of a full size antenna. Fox and Li (11) have shown that lasers operate in basic cross-sectional modes. Each mode has different associated

Figure 6. Helium-neon gas laser

(a) without light shield

(b) with light shield

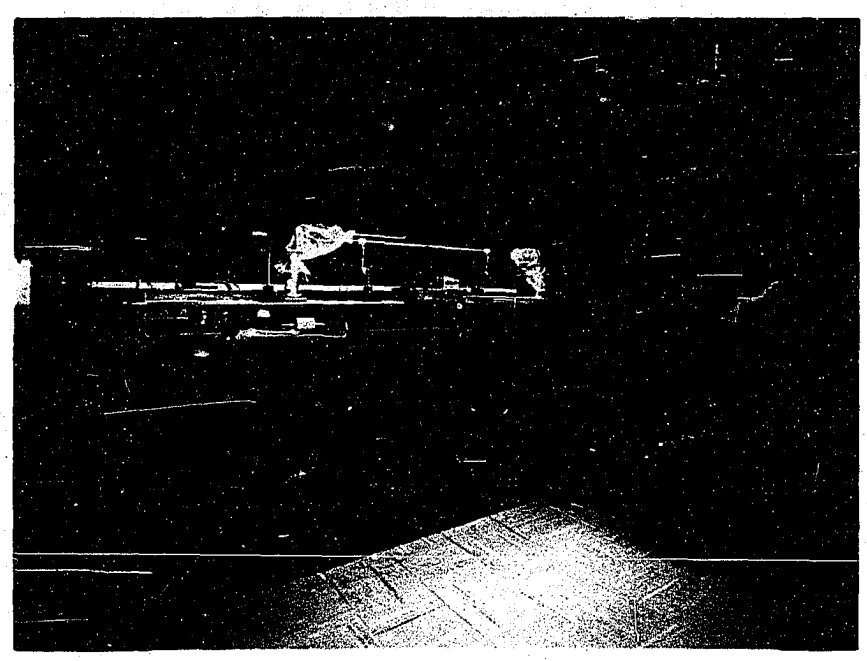

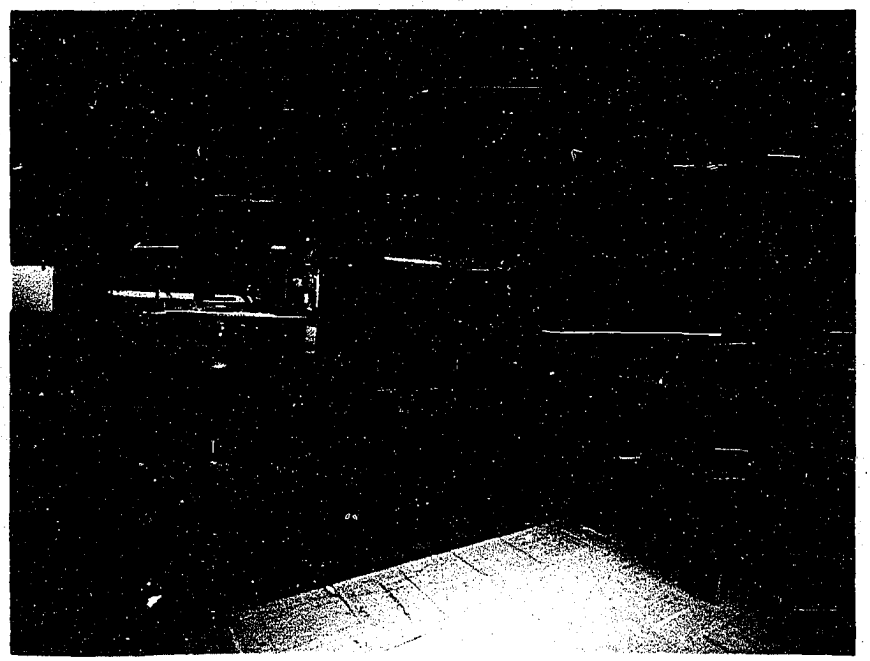

losses and as a result each has a certain gain threshold which must be exceeded in order that the laser operate in this mode. The modes are characterized as TEM_{mn} modes with the lowest inherent losses associated with the TEM_{00} mode. The next lowest is the TEM_{01}. Several low order modes are shown in Figure 7.

The desirable mode is the TEM_{00} since it has uniform phase across the entire wave front. All higher order modes have phase reversals and associated nulls across the wave front. In order to obtain the desired plane wave output, the laser must be forced to operate in the TEM_{00} mode. This mode can be obtained using either the confocal or hemispherical configuration (2). When using the confocal configuration an optical stop must be used to restrict the cross-section of the cavity. The cross-section must be kept to a relatively small value and the stop must be accurately centered in the cavity. The hemispherical configuration presents no problems of this type and higher power outputs are possible through the use of more of the active region of the discharge.

The diffraction losses of the hemispherical cavity are strongly affected by the mirror separation. For mirror separations greater than the radius of curvature of the spherical mirror, the diffraction losses are extremely large and laser action cannot be obtained for any mode. As the mirrors are moved together the diffraction losses

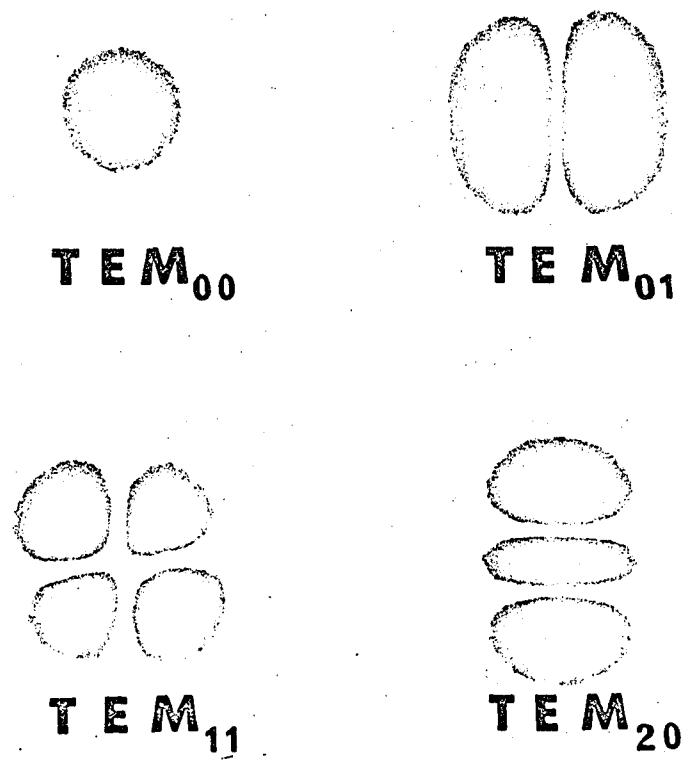

Figure 7. Intensity distributions for low order cross-sectional modes

decrease. When the losses have decreased sufficiently, laser action begins for the mode with the lowest threshold. This is normally the TEM_{00} mode. It is possible, however, to increase the diffraction losses for this mode without changing them for the TEM_{01} mode. For example, a speck of dust located at the center of the beam creates large scattering losses for the TEM_{00} mode, but since it occurs at the null of the TEM_{01} mode it does not affect the losses of this next higher mode. It is even possible to generate the higher order modes by inserting into the cavity fine wire which will change the losses, thereby favoring one mode or another. Thus, care must be taken to guarantee the cleanliness necessary for TEM_{00} mode operation.

As the mirrors are brought still closer together, the diffraction losses continue to decrease and eventually higher order modes begin to appear in the output. It is easy to check the effectiveness of the attempts at cleanliness by observing the difference between the mirror distances for laser action to just begin and the point where higher order modes begin to appear. In a typical case, the mirrors could be moved closer together by 2 cm after laser action begins until higher order modes begin. Since the losses change considerably as the mirror separation is changed, the output intensity can be controlled in this manner. It is also possible to control output intensity by varying the excitation. The output was monitored

photoelectrically and maintained at a constant level. The photoelectric detector could be used to measure variations of 2% in the output intensity.

It was found that the laser should be turned on at least an hour before measurements are made. This is necessary for two reasons. During the initial hour the transmitter power output tends to gradually rise. This gradual rise can be controlled but requires constant attention. The second reason is that the laser discharge tube temperature rises considerably during the initial minutes of operation. As the plasma temperature increases it is necessary to adjust the alignment of the mirrors. Maintaining mirror alignment after the laser has reached operating temperature is no problem. Once the mirrors are adjusted for maximum output no further adjustment is necessary for a period of several hours. Measurements were always taken at night to minimize effects of line voltage fluctuations and vibration present in the building during the day. On all occasions, the laser output was monitored before, during, and after a photographic recording to insure proper operation.

The laser output for the TEM_{00} mode is slightly diverging due to the lens effect of the spherical mirror and the nature of the mode. For the laser used the divergence is about one-third degree. In order to obtain plane waves from the laser to illuminate the aperture, two lenses of

relatively short focal length were used. The first lens focused the beam to a point. The second lens was then positioned such that its focal point coincided with this point. This results in a collimated beam. The beam still spreads due to diffraction but at a negligible amount for this experiment.

The desire to have a collimated beam stems from two reasons. First, and most importantly, the collimated beam has essentially a constant intensity at all distances. This allows one to move the aperture along the beam maintaining a constant illumination level. Secondly, it is desirable to have a plane wave with constant phase across the wave front to illuminate the aperture. This is not especially important since the fields of interest are beyond the horizon and the source configuration has only a small effect on these fields. At any rate, the phase variation would be quite small, since the aperture is a small fraction of the beam cross-section.

The mirrors used reflect better than 99% of the light at 6328 Å; however, they transmit large amounts of blue light. This blue light is not coherent or monochromatic and diverges quite rapidly. Since the film used as a detector is sensitive to blue light it was removed with a narrow band spectral filter. The filter used is centered at 6330 Å and has a pass band of 100 Å.

The laser discharge tube was enclosed in a small curtained box to contain, as much as possible, the strong background light. This allowed the room containing the laser to be maintained quite dark. Both ends of the laser were external to this curtained box to allow access to the mirror adjustments. The curtaining material was not completely opaque and there were ventilation holes through which light escaped. Thus, it was necessary to make all measurements within another curtained area. The area where the measurements were made was well isolated from the intense light of the laser discharge tube. A plywood screen was used to eliminate the direct light travelling from the discharge tube toward the enclosure.

Mounted on this plywood screen was a shutter. The shutter was capable of calibrated exposure settings from 1/25 sec to 1/100 sec. It also was capable of time exposures of arbitrary lengths. An electro-mechanical device was constructed to allow the shutter to be operated electrically. It was controlled by a clock which permitted automatic time exposures ranging from 1 second to 1 hour.

The aperture, which simulated an antenna, was a circular hole drilled in 1 mil brass. The hole was viewed microscopically and found to be very well formed. It was found on earlier apertures that on occasions burrs were left on the hole and sometimes the hole was not truly

circular. This hole was perfect in all visible respects. The diameter, as measured with a stage micrometer, was 2.3 mils.

The aperture was cemented to an aperture mount. The mount, made of aluminum and wood, was padded with felt where it was in contact with the pyrex disc. A spring held the mount lightly against the surface. Holding the spring was an arm fastened to the disc support. The arm was constructed to permit positioning of the aperture at any point on the surface. The spring maintained a constant pressure on the felt for all positions of the aperture on the surface and thus, a fixed aperture distance above the surface. This distance above the surface is the transmitter altitude. It was measured by positioning a tapered wedge to just interrupt the laser beam coming through the aperture. The thickness of the wedge at that point was then measured with a micrometer. Aperture height was determined to be 72 mils. The side of the aperture facing the photographic film was covered with special black felt paper furnished by the Eastman Kodak Company. This paper is highly absorbent and prevents light scattered off the photographic material from being reflected back onto the film. The remaining surfaces were sprayed with a flat black paint.

The collimated laser beam, approximately 150 mils in

Figure 8. Aperture mounted on earth model as viewed from (a) source side

(b) receiver side

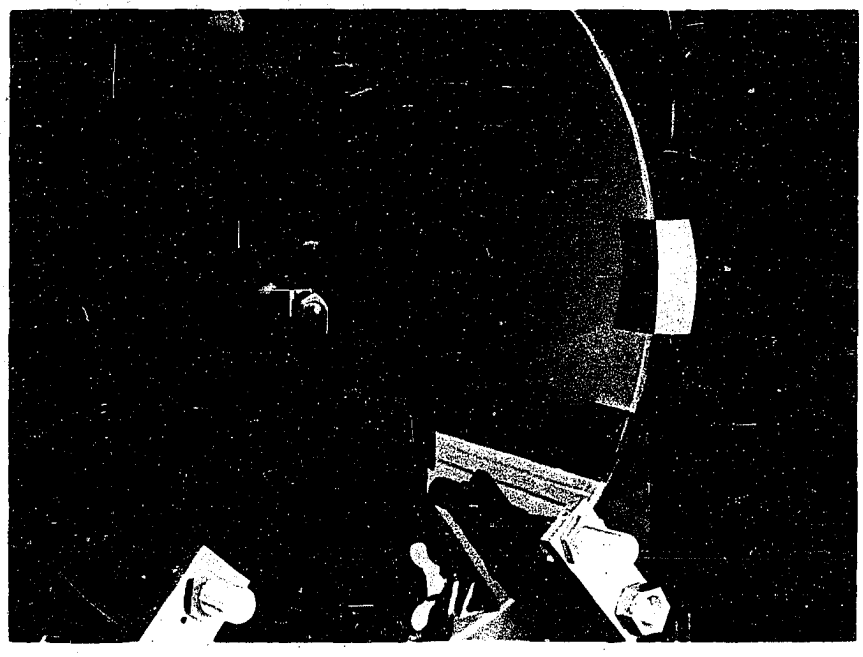

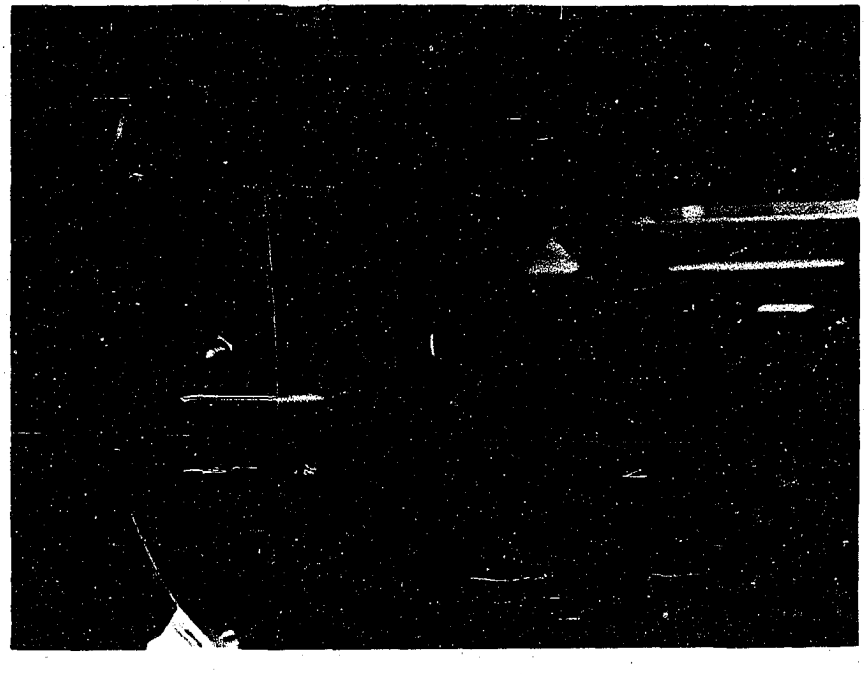

diameter, was directed onto the back side of the aperture. Since the aperture is 2.3 mils in diameter, only a small fraction of the laser beam is used. One reason for not using a smaller beam diameter is that the intensity from the center of the beam varies according to the Gaussian function

$$I(\rho) = I_o e^{-\frac{4\rho^2}{D^2}} \qquad (25)$$

where ρ is the radial distance from the center line of the cavity and D/2 is the value of ρ at which the intensity has fallen to 1/e of its central value I_o. It is necessary to have a beam diameter several times larger than aperture size to maintain a constant intensity over the aperture. A larger beam diameter makes centering of the aperture in the beam much less critical.

To center the aperture within the beam a strong light was placed on the side of the aperture opposite that of the laser. Several neutral density filters were used to reduce the laser beam intensity. With the reduced laser intensity and the strong white light coming through the aperture, the aperture was easily visible and could be centered within the laser beam.

Typical power outputs for lasers of the type used operating in the TEM_{00} mode vary from fractions of a milliwatt up to one milliwatt maximum. Since it is difficult

to maintain TEM_{00} oscillation at maximum output, the monitored output was maintained at two-thirds the maximum value. Since the aperture intercepts approximately 1/5000 of the beam area, the transmitted power is approximately 0.1 to 0.2 μ watts. The great value of the gas laser lies in its ability to generate continuously large amounts of monochromatic and coherent power at optical frequencies. No other optical source can match its performance.

The circular aperture produces a characteristic circular diffraction pattern whose central maximum is easily visible at distances of 30 inches. This is very fortunate since the aperture can be visually aligned to aim at the horizon. As the aperture output is moved in elevation, the beam goes from a reflected one to one that misses the surface altogether. Intermediate to these two positions, there is one which consists of both reflected and direct line of sight transmission. The beam is adjusted to give this intermediate condition. It has been found that fields beyond the horizon are not strongly affected by aiming of the source so long as the horizon intercepts approximately the center of the transmitted beam.

B. Analog Model of Terrestrial Surface

The model used in these experiments was a pyrex disc made especially for this use. It was manufactured by Optics

for Industry, Milwaukee, Wisconsin. The disc is made of commercially annealed pyrex #7740. It was constructed from two discs of 1-1/4 inch thick pyrex twenty-four inches in diameter glued together with black epoxy cement. The epoxy cement is opaque and highly absorbent of incident light. One surface was polished to a radius of curvature of 18 feet forming a convex surface accurate to 1/2 wavelength or 1/4 micron in any six inch region. Thus, the surface is a section of a sphere with an 18 foot radius, not deviating from the true radius by more than two wavelengths, or one micron, over its entire surface.

If the surface is used to represent a section of the earth, the scale factor is:

$$\text{earth scale factor} = \frac{\text{earth radius}}{\text{model radius}} = \frac{20.87\text{x}10^6\text{ft.}}{18\text{ ft.}} = 1.16\text{x}10^6 \quad (26)$$

Then the variation of one micron corresponds to hills on the earth of 1.2 meters or 4 feet. The two foot diameter of the disc corresponds to $2.3\text{x}10^6$ feet or 440 miles over the earth's surface. The approximation made by Pryce that the earth is a smooth sphere holds true in this analog model better than it ever does for the earth.

Some preliminary data were taken using a plywood and fiberglass model made in the Electrical Engineering Department shop. This surface was rough and hilly and the effects of the hills were visible in the qualitative results

Figure 9. Earth model mounted in holder

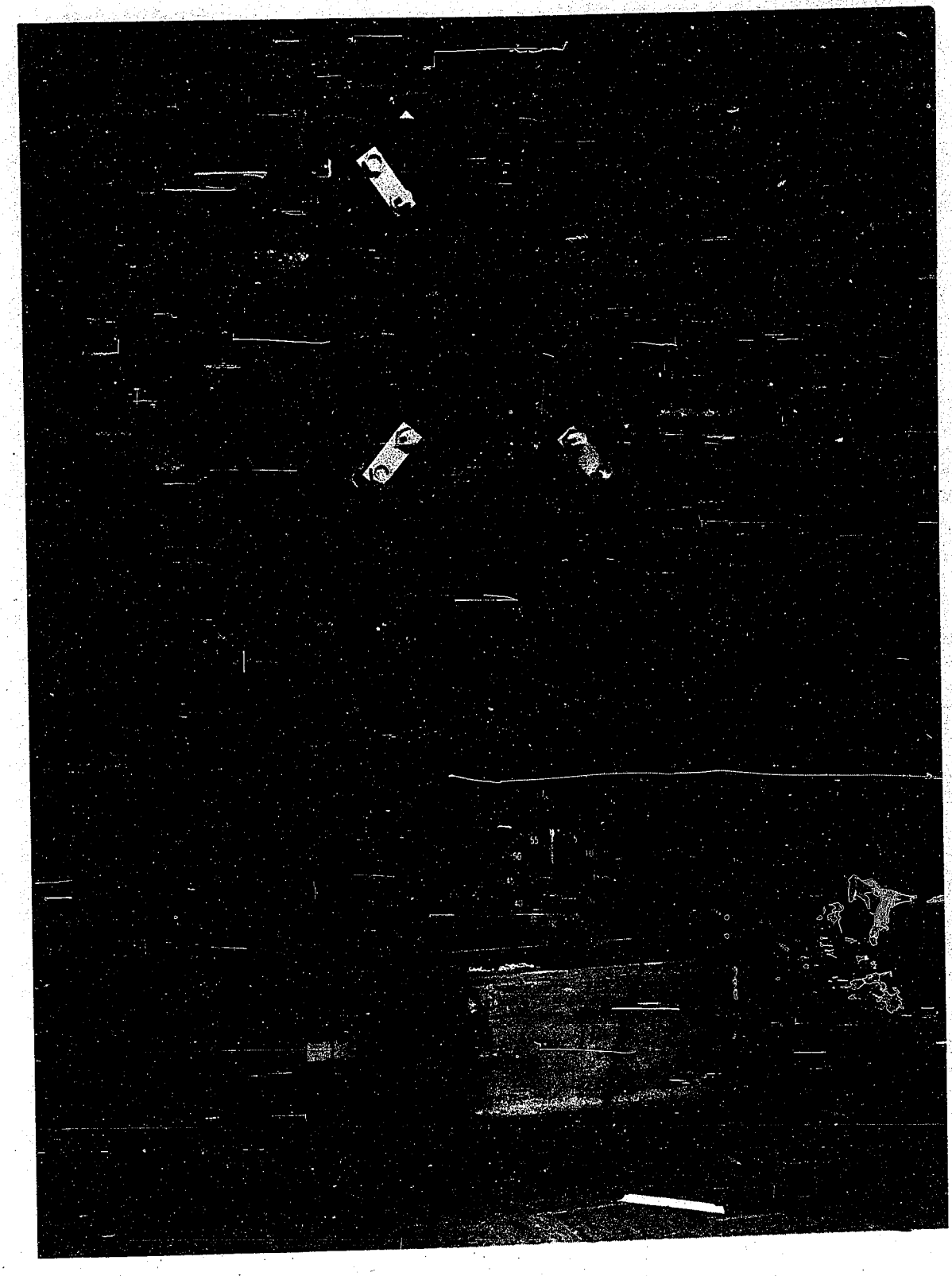

obtained. No quantitative measurements were made using this surface since the aperture height above the true sphere surface (above sea level) and the actual radius of curvature of the surface were not known. As the aperture was moved to effect variations in range, changes in altitude could off-set range variations. Results obtained from this plywood and fiberglass disc would have been valid for the particular case of hilly terrain but would have been very difficult to correlate with theory. When using the pyrex disc the problem of maintaining a known antenna height above the true sphere surface for different ranges and from one experimental run to the next was simply a problem of maintaining the aperture a fixed distance above the pyrex surface.

The pyrex disc was mounted vertically in a sling with three spring loaded contacts to position the mirror around two axes. The weight was supported by two steel tee beams which were attached to a 300 pound block of cement for stability. The entire mount was quite rigid and very stable.

Black flannel draw curtains hanging from the ceiling enclosed the disc in a 10 ft. by 10 ft. dark room within the larger room. The curtain material is highly absorbent of incident light. The walls of the entire room are painted black and several large black plywood panels form light

baffles. The major background light comes from the laser discharge tube. This light is reduced to a negligible amount by use of additional curtaining material to enclose the laser. Background light within the curtained area containing the disc was demonstrated to be negligible with several one hour exposures using Panatomic X sheet film. This film, when developed, contained no evidence of exposure from background light. It is necessary to have a good dark room since the film is exposed to background light during the entire time it is exposed to the laser light.

Some light from the aperture incident on the film is scattered. Everything capable of intercepting this scattered light is protected with absorbent material to prevent its reflection back on to the film. In working with the rough plywood-fiberglass model it was found that light scattered off the film was scattered by the disc back onto the film. This could be eliminated by positioning the film so that only the very weak fields were intercepted by the film. This required, however, that the recorded fields be located at the very edge of the sheet of film. It was then necessary to process the film protecting the normally unused edges. The smooth polished pyrex disc presented no such problem. Any light scattered off the film was reflected away from the sheet of film onto absorbent material.

Air circulation and turbulence was a minimum in the

enclosed area since there was no place for air to enter or leave except through the curtain material.

At this point, the validity of representing the interior of the earth by the interior of the pyrex disc will be considered. There are two basic properties of the interior of the earth of importance, the dielectric constant and the conductivity. Gerks (13) gives the values:

Sea water	$\epsilon_e = 80$	$\sigma = 4$ mho/m
Good soil	$\epsilon_e = 30$	$\sigma = .02$ mho/m
Poor soil	$\epsilon_e = 4$	$\sigma = .001$ mho/m

Two approximations are made regarding the interior of the earth in Pryce's theory. The first is that all fields decay exponentially interior to the earth sufficiently fast to guarantee that effects of inhomogeneities can be neglected. Any inhomogeneity would cause a reflected wave to travel back to the surface. Even if the earth were homogeneous, if the waves were unattenuated, energy would be reflected from the surface on the other side of the sphere, producing a standing wave interior to the earth. Pryce's theory neglects the effects of any energy reflected from other than the homogeneous surface. In the case of the pyrex disc, light entering the surface is unattenuated since the absorption of the pyrex is quite low. Light entering the pyrex is not reflected back to the surface, however, since the

pyrex is very homogeneous until the junction of the two sheets. At this point is the highly absorbent epoxy cement. Thus, energy entering the pyrex is absorbed and not returned to the surface. The only energy incident on the film is that from the aperture reflected from the homogeneous surface.

The second approximation is one which only sometimes holds for radio propagation over the earth. This is the approximation that $T = 0$. The assumption that $T = 0$ simplifies considerably the solution, in that the roots of Equation 17 become the zeros of the Airy integral as given by Equation 23. $T = 0$ also simplifies the height-gain functions as given by Equation 24. The exact solution for a_s can be written in the form of an infinite series.

$$a_s = a_{s,o} + T - 1/3\, a_{s,o}\, T^3 - \ldots \qquad (27)$$

for small values of T, where $a_{s,o}$ are the zeros of the Airy integral. T is a measure of the reflection taking place at the surface. Recall that for vertical polarization

$$T_1 = -i \frac{\epsilon'}{K(\epsilon'-1)^{1/2}} \qquad (20)$$

and for horizontal polarization

$$T_2 = \frac{-i}{K(\epsilon'-1)^{1/2}} \qquad (21)$$

where

$$\epsilon' = \epsilon_e - i \frac{18000\ \sigma}{f_{mc}} \tag{7}$$

For the case of the pyrex disc $\epsilon_e = 1.474$ and $\sigma \approx 0$ so $T_1 = -i(.0071)$ and $T_2 = -i(.0048)$. For the earth scale factor as given by Equation 26 the laser corresponds to a 400 Mc transmitter. Referring to Figure 3 for vertical polarization, this value of T_1 is seen to correspond almost exactly to the case of propagation over poor soil at 400 Mc. Figure 4 shows that the assumption that $T = 0$ for horizontal polarization is not as good as it is in the case of the actual earth. The difference is almost entirely due to the difference in dielectric constant as can be seen by using Equation 7 and the values for ϵ_e and σ given by Gerks to calculate the complex permittivity. At 400 Mc, this gives

$$\epsilon' = 30 + i\ .9 \approx 30 \qquad \text{good soil}$$

$$\epsilon' = 4 + i\ .045 \approx 4 \qquad \text{poor soil}$$

Thus, the reflection is essentially due to the dielectric constant change and the conductivity has a negligible effect. The conductivity in the case of sea water does play a role in the reflection; however, for soil the conductivity is only necessary to damp the inwardly travelling energy. The pyrex disc does not damp the inwardly

travelling energy, but absorbs it when it reaches the epoxy cement joint.

The approximation that $T = 0$ is worst for the smallest value of $a_{s,o}$. This is when $s = 1$, the first root, and the value is

$$a_{1,0} = 2.3381$$

Setting $a_1 = a_{1,0}$ is an error of less than 1/2% and is felt to be negligible for this study.

C. Detector of Electromagnetic Energy

Early in this research, attempts were made to use a photomultiplier with a fiber optics bundle to detect the energy at the receiver location. It was soon found that, though the photomultiplier would respond to light in the region where no light was visible, the resolution and sensitivity were not good enough for quantitative measurements of height-gain or range functions. Had the experiment been concerned with transmission paths in the region above the horizon, it is possible that a photomultiplier would have been a satisfactory detector. However, it is felt that the advantages of photographic recording far outweigh its added complications. All results presented in this work were obtained photographically.

Photographic film was placed in contact with the edge of the pyrex disc such that the transmitted beam from the

aperture struck the film. The film used was four inches wide and three to five inches long, permitting considerable region on either side of the beam to be recorded. The film extended out past the front edge by about one-half inch in one set of measurements and by about two and one-half inches in another case. It also extended about one inch beyond the rear surface of the pyrex disc. A mount was constructed and fastened to the disc which held the film in place while an exposure was made.

A small light bulb was mounted within a camera placed behind the disc. When the shutter of this camera was opened, the light from the bulb illuminated the film extending beyond the rear edge of the disc. Since the edge of the disc was opaque, the film contained a step change in exposure at the back edge of the disc. This reference mark was placed on every sheet of film by tripping the camera shutter for one-tenth second after the film was placed in the holder. The laser then automatically illuminated the aperture exposing the film to the variations in field intensity to be measured. Several sheets of film were exposed uniformly over the area extending past the front surface. These sheets had two steps, one corresponding to the rear edge and the other corresponding to the front edge. By measuring the distance between these two steps the thickness of the disc could be accurately determined. It was measured to be 38.27 mm with agreement in

all cases within 50 microns. It should be noted that measurements of the thickness of the disc using glass photographic plates gave the same values as the sheet film did. Thus, when the pattern corresponding to variations in the magnitude of the transmitted field intensity was scanned and referenced with respect to the rear surface, it could be converted to variations with respect to the front surface.

In choosing the film to be used, several factors must be considered. Since the fields beyond the horizon were primarily of interest, the photographic material must be capable of accurately reproducing these weak and rapidly changing intensities. When light strikes a photographic emulsion, it produces changes in the individual grains of silver halide which cause the effected grains to be reduced to silver under the action of a developer. The resulting grains of silver permit the negative to transmit less light where the concentration is highest. Photographic density has been found to be a good measure of the exposure an emulsion has received and is defined as:

$$D = \log_{10} Op = -\log_{10} tr \qquad (28)$$

where Op is the opacity of the film

and tr is the transmittance.

Exposure is defined as

$$E = I \times t \tag{29}$$

where I is intensity

and t is time.

When photographic material is given a series of exposure steps, in which each exposure differs from the preceding one by a known amount, the resulting negative has a series of steps differing in density or blackness. From a negative of this type a relationship can be obtained between density and exposure. The results are usually plotted as density versus the logarithm to the base 10 of exposure. Such a characteristic curve, often called the "H and D curve" after Hurter and Driffield, is shown in Figure 10. Several important characteristics can be obtained from a curve of this type. First, it is seen that a certain minimum exposure is required in order to affect the film. For exposures less than this minimum value, indicated by point A on the curve, no image density results. For exposures greater than point A, the image has a measurable density and exposure differences result in density differences. The region from point A to point B is called the toe of the curve and is characterized by increasing slope or gradient. From point B to point C, the gradient is constant and density increases as a linear function of the logarithm of exposure. For quantitative measurements, it is desirable to operate in this region. Above point C, the gradient

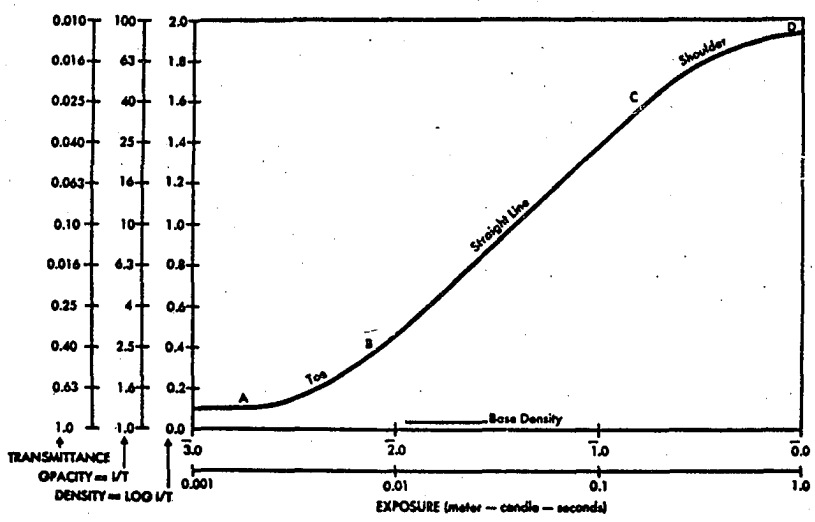

The Characteristic Curve.

Figure 10. The characteristic curve for photographic material

decreases for increases in exposure as saturation of the film sets in. This region is called the shoulder of the curve. The slope of the characteristic curve at any point is called gamma. The difference in exposure resulting in a change in density from toe to shoulder is known as the linear exposure scale, or latitude, and is a measure of the maximum variation in field intensity which can be measured by the film for a single exposure time. Changing the exposure time results in different intensities in the linear region and the linear exposure scale can effectively be increased.

The light-sensitive photographic emulsion consists of crystalline grains of silver halide, mostly bromide, suspended in gelatin (23). Several important relationships are known about these grains and the properties of the emulsion. The first is that the grains primarily respond to violet and blue light. In order to obtain sensitivity to light other than blue, sensitizing dyes are used. There are several regions of the spectrum covered by basically different dyes. The most commonly used classifications are blue sensitive, orthochromatic (blue and green), panchromatic (blue, green, and red), ultraviolet, and infrared. Of these classes, the only satisfactory one for this experiment is panchromatic film. A second relationship is that as grain size increases the speed of the film increases.

Thus, to measure weak fields a high speed film with relatively large silver halide grains would be desirable. However, increasing speed has the disadvantages of increased granularity and decreased resolution and acutance. The exact manner in which these factors are interrelated is very complicated and there are still no clear relationships which exist.

Resolving power and acutance are measures of the ability of film to go from one density to another in very short distances. Acutance, while directly related to the maximum rate of change in density per unit length on an emulsion, has the disadvantage of being very difficult to measure and highly dependent upon development. For this reason, Kodak does not publish acutance values for their film. They do place film in the rather general catagories of Low, Medium, High, and Very High. Panatomic X sheet film, from which most results were obtained, rates High.

Resolving power measurements are more reproducible and listings are given of Low, Moderately Low, Medium, High, Very High and Extremely High. Panatomic X rates High, which means a resolution of 96 to 135 lines per millimeter. Direct correspondence with the manufacturer verified that for the type exposures taken in this experiment the expected resolution would be 100 lines per millimeter. It was desirable to record the fields by gradients in density of 1.0 per

200 microns or less for convenience of measurement and so as not to exceed the response of the film. Since the theory predicts that the fields will change by approximately 10 db in 270 microns, gamma should be as low as possible and certainly less than 1. The value of gamma is highly dependent upon film, developer, temperature of developer, amount of agitation, and time of development. The highest practical gammas are of the order of 5 and the lowest are about 0.3.

Film is classified as to its contrast characteristics. For all else equal, high contrast film, when developed, has a much higher gamma than low contrast film. For example, while Panatomic X sheet film normally might have a gamma of 0.5 for 6 minutes of development, Kodak Type M plates, under the same conditions could be expected to have a gamma greater than 1.0. Thus, a film with low contrast characteristics, high resolution and acutance, and fine grain properties is desired. Panatomic X sheet film is suitable in all respects.

The desire for low gamma also affected the choice of developer. Some developers are more active than others. As seen in Figure 11, for the same conditions, different developers give different gammas. The most important commercial developing agents are metol and hydroquinone. In addition to the developing agents, developers contain an

Sensitometric Curves: For average product and average processing.

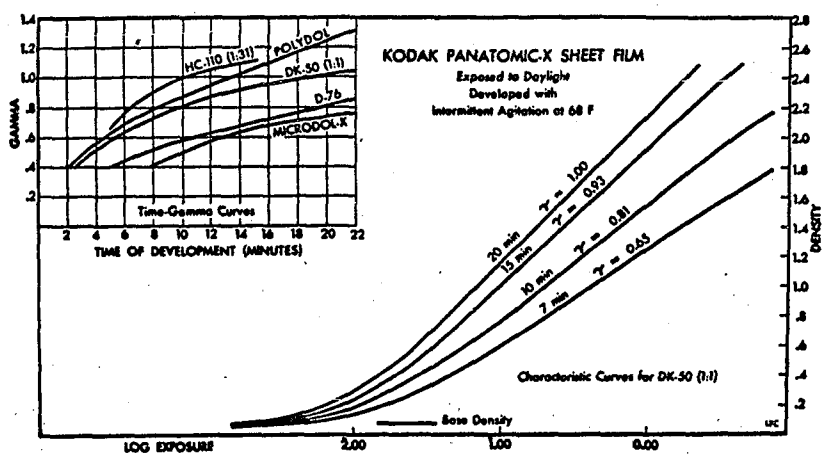

Figure 11. Sensitometric curves for Panatomic X sheet film

alkali, as an accelerator, to make the developing agent active. The activity of the developer depends upon the concentration of the developing agent, the effective alkalinity of the solution, and temperature. Kodak Developer D-76 with its mild alkali, borax, has a much slower rate of development than D-19, which contains sodium carbonate. Temperature of the developer affects the rate of development by changing the speed at which the reaction takes place. Lower temperatures result in longer development time for the same gamma. Because of its mild activity and general usage D-76 was chosen. Another suitable developer would have been a fine grain developer such as Kodak Microdol X. The longer a sheet of film remains in a developer, the more the reaction takes place until all exposed grains are developed. Therefore development time affects the degree of development and thus, gamma. As can be seen in Figure 11, for longer development times gamma increases to a maximum value known as the saturation gamma for the developer-film combination.

With use, the strength of a developer decreases, partly because of the destruction of the developing agent in changing exposed silver halide to metallic silver, but primarily because of the restraining effect of the accumulated reaction products. As a developer diffuses into a photographic emulsion it encounters exposed silver halide crystals. Some of the developer is used to reduce the surface crystals,

exhausting somewhat the developer and producing reaction products. Some of these reaction products diffuse out of the gelatin and some continue inward with the developer. These reaction products have a strong retarding effect on the reduction of exposed silver halide to silver. As the reaction continues to produce a visible image in the form of silver, it continues to produce reaction products. Agitation brings fresh developer into contact with the emulsion surface, accelerating development and mixing the reaction products with the bulk of the developer.

Film is available as rolls, sheets, and plates. Because of the method used to photograph the fields, roll film could not be used unless cut into strips. One of the advantages of working with sheet film is the ability to develop many sheets at one time. The film was placed in hangers and ten sheets were developed at one time in a gallon tank of developer. To avoid problems with exhaustion of developer, fresh developer was used for each batch of ten sheets. Since each sheet experiences the same conditions of development, very consistent and uniform results were obtained. The glass photographic plates were developed in a tray which held only one plate. The values of gamma were not as consistent for the plates as for the sheet film, since each plate was developed individually. It was possible because of the size of the plates to have two exposures on a single plate. Since each exposure can be for a

different exposure time, gamma can be obtained for each individual plate as will be shown in the next section.

It is known that reaction products are heavier than the developer and tend to flow over the sheet of film. Because of this, special care must be taken to guarantee that uniform development occurs over the entire sheet. The most important part of the processing step to guarantee uniform development is agitation. Eastman Kodak (25) recommends that sheet film developed with hangers in tanks be agitated with a particular motion and at definite intervals. Insufficient or improper agitation results in streaks on the negative due to reaction products. Excessive agitation results in higher densities at the edges of the sheet and spots of uneven development. When using hangers, constant agitation must be avoided if a high degree of development uniformity is desired. The reason for this is that when using hangers, constant agitation results in patterns of developer flow over the sheet which are non-uniform, giving non-uniform development. On the other hand, when it is possible to insure uniform motion of the developer over the entire negative, as in the case of plates, it is desirable to use constant agitation. With increased agitation developer strength must be cut by dilution or time of development reduced to maintain a low gamma.

When a sheet with an abrupt change in exposure is

processed, several new effects appear. These effects, known as adjacency effects, have long bothered the spectroscopist with narrow spectral lines on a clear background and the astronomer with bright stars superimposed on a clear field. The cause of adjacency effects is that when a region of heavy exposure lies next to a region of little exposure, development takes place faster at the edge of the heavy exposure than within the exposure. Within the heavy exposure developer is used up as fast as it proceeds inward, accumulating reaction products which, in turn, reduce the effectiveness of fresh developer as it arrives. In the region of little exposure, developer proceeds inward to the support material with little loss of strength. Now begins a transverse diffusion in the gelatin of fresh developer from the region of little exposure into the region of heavy exposure. Reaction products also diffuse from the dark to the light area. The edge of the dark region has fresh developer diffusing in from the surface as well as from the adjacent region and thus, this region develops faster. Attempts to obtain low gammas result in an aggravation of this problem, since reducing development time reduces the development elsewhere more than at the edges. Vigorous agitation reduces adjacency effects, but since it causes development to proceed at a faster rate, it results in shorter development times for the same gamma,

which tends to reduce the improvement.

Relatively large adjacency effects were observed in this experiment. These adjacency effects result in a gamma, in the region of interest, 20% greater than gamma measured with a step tablet. Thus the use of a step tablet to evaluate gamma was not very successful. The use of a step tablet did prove to be a convenient method to compare different film and the effects of agitation, development time, and developer changes. The next section develops a method for measuring gamma in the region of interest, independent of the step tablet.

Temperature control is necessary, not only because the rate of development is strongly affected by temperature, but also because large temperature changes from one bath to another can introduce stresses in the gelatin which result in a loss in position accuracy. The temperature of all baths was maintained at 68° F. Developer was mixed at the end of the previous day and allowed to sit in the rinse water overnight to stabilize at 68° F. This same water bath was used to cool the fixer and rinse the film. After water rinsing, the film was rinsed in Kodak Photoflo, which is a strong wetting agent. This resulted in uniform wetting of the gelatin, which is necessary to insure uniform drying. As film dries, the gelatin shrinks. Uniform drying insures uniform shrinkage. Kodak estimates that normal shrinkage of sheet film due to processing does not exceed 0.1%. By

comparing sheet film results with that obtained using photographic plates, dimensional stability has been shown to be no problem.

IV. ANALYSIS OF RESULTS

The qualitative results obtained show that a diffraction pattern is produced corresponding to a circular aperture with very well defined nulls superimposed on what appears to be the diffraction of a straight edge. The effect of curvature is seen as a smearing of the reflected spot into a section of an ellipse. The aperture size, as calculated from the diffraction pattern, was 2.2 mils. This compares well with the 2.3 mils measured with a stage micrometer.

The quantitative results rely on the use of the linear region of the "H and D curve" as shown in Figure 10. In the linear region, gamma is a constant and therefore

$$D_2 - D_1 = \gamma \left[\log_{10} E_2 - \log_{10} E_1 \right] \tag{30}$$

Exposure is the product of intensity and time, and intensity is proportional to the square of the magnitude of the electric field strengh, so the above equation can be rewritten as:

$$D_2 - D_1 = \gamma \log_{10} \frac{I_2 t_2}{I_1 t_1} = \gamma \left[\log_{10} \frac{|\mathcal{E}_2|^2}{|\mathcal{E}_1|^2} + \log_{10} \frac{t_2}{t_1} \right] \tag{31}$$

Since the intensity at a particular altitude is a constant, gamma can be evaluated by taking exposures of different exposure times and comparing densities at the

same altitude. This gives, from Equation 31, that

$$\gamma = \frac{D_2 - D_1}{\log_{10} \frac{t_2}{t_1}} \tag{32}$$

This very important relationship allows one to determine gamma in the region on the film where measurements are being made. Thus, any adjacency effects are included in the measurements of gamma. Exposure times of one, five, and thirty minutes were used to measure fields at a point and there was no problem in evaluating gamma by this method. Good agreement on a value of gamma was obtained between different exposures as long as they had been processed together.

Equation 31 can be rewritten to give the relative field strength at point 2 in db as:

$$20 \log_{10} \left|\mathcal{E}_2\right| = \frac{10}{\gamma} D_2 + \left[20 \log_{10} \left|\mathcal{E}_1\right| - \frac{10}{\gamma} D_1\right] - 10 \log_{10} \frac{t_2}{t_1} \tag{33}$$

The quantity in brackets is evaluated for a particular point on the film corresponding to some reference altitude. The only restriction on the choice of this point is that it must occur within the linear region of operation (region of constant gamma), which is the valid region for Equation 30.

This quantity in brackets is a constant related to the sensitivity of the film and the intensity of the laser, among other things, and is chosen to give agreement between theory and experimental results at this reference altitude. Because of the nature of the photographic process, exposures greater than zero can still result in zero density, and for this reason it is necessary to introduce this constant. It remains the same for all sheets of film within a batch, but may change slightly from one batch to another as the sensitivity of the film may vary slightly.

For a particular negative, the exposure time is constant over the entire sheet and in this case, Equation 33 becomes:

$$20 \log_{10} \left| \mathcal{E}_2 \right| = \frac{10}{\gamma} D_2 + \left[20 \log_{10} \left| \mathcal{E}_1 \right| - \frac{10}{\gamma} D_1 \right] \quad (34)$$

The value of the field at point 2 on a negative is related to the field at the reference point by the change in density between Points 1 and 2. Negatives were scanned using a Jarrell Ash High Precision Recording Microphotometer, Model 23-500. This machine is capable of scanning a negative with slit widths as small as one micron and as short as 10 microns. Over a distance of 200 mm it maintains a positional accuracy of one micron. When recording data with this machine a slit width of 10 microns and a length

of 100 microns was used. This is analogous to an averaging of the measured fields over a vertical distance of only 40 feet. Scan speed was 1 mm per minute. Several negatives were scanned with narrower slit widths and the results were observed to agree with the wide slits. Since lower amplifier gain is required and smoother results are obtained with the wide slits, they were used.

Typical photographs of different exposures are shown in Figures 12 and 13. Unfortunately, the reproduction process lacks the resolution to show the detail available in the original negatives. The microphotometer was used to scan the negatives in the region corresponding to transmission of the main beam beyond the horizon. The output was recorded continuously in terms of percent transmission with a strip recorder. Data points were read from this recording for every 40 microns on the film, corresponding to altitude changes of 160 feet. These were converted to density and Equation 34 was used to obtain the fields from these densities. A typical height-gain plot obtained in this manner is shown in Figure 14. Data points are shown for a 5 minute and a 30 minute exposure. The weakest fields recorded with a 5 minute exposure are seen to be about 15 db below the free space field. Thirty minutes exposures are able to record fields almost 25 db below the free space field strength. Since a 30 minute exposure is the

Figure 12. Typical field patterns

Figure 13. Typical field patterns

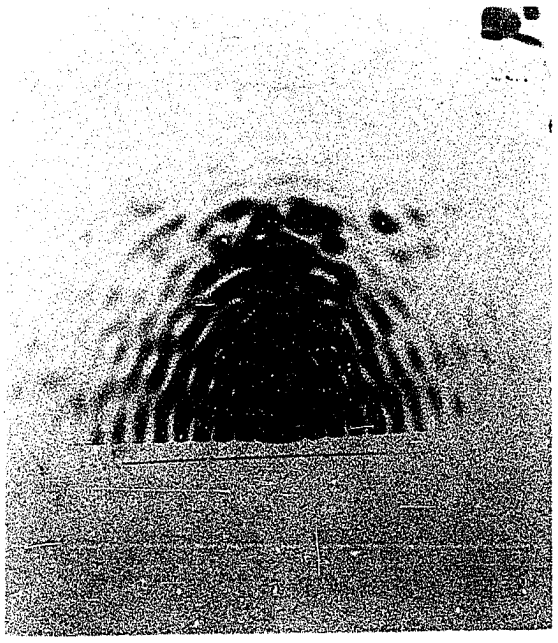

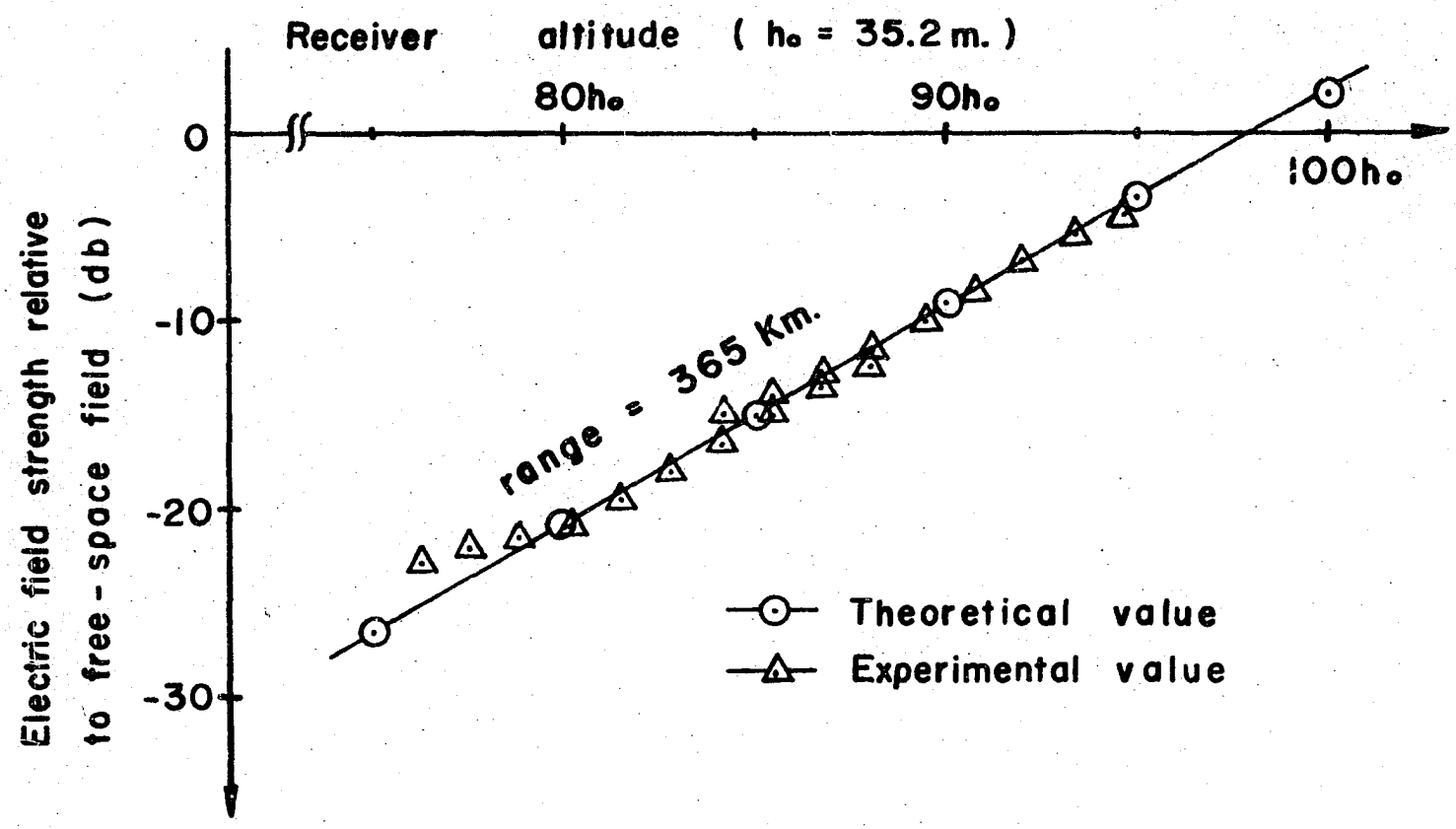

Figure 14. A typical height-gain function
(transmitter altitude = 61 h_0)

longest exposure that can be taken conveniently, the weakest fields recorded are 25 db below the free space field. For the particular combination of range and transmitter altitude this limits the field strength measurements to above $75h_o$ or 6700 feet.

Included in Figure 14 is a plot of the theoretical values predicted by Equation 13 when the series is evaluated for the first five terms. The use of just the first term results in an error since at the altitudes considered, higher modes begin to be significant. A computer program which evaluated the series for five terms was written, and using Domb's (9) values for height-gain functions of individual modes, curves were obtained for different ranges. Typical results of this program are shown in Figure 15. Figure 16 is a plot of photographic results for several different ranges. From this figure, it is possible to estimate the range attenuation by measuring the vertical separation of the curves. Results using this technique are shown in Figure 17 along with the theoretical values as predicted by Equation 13.

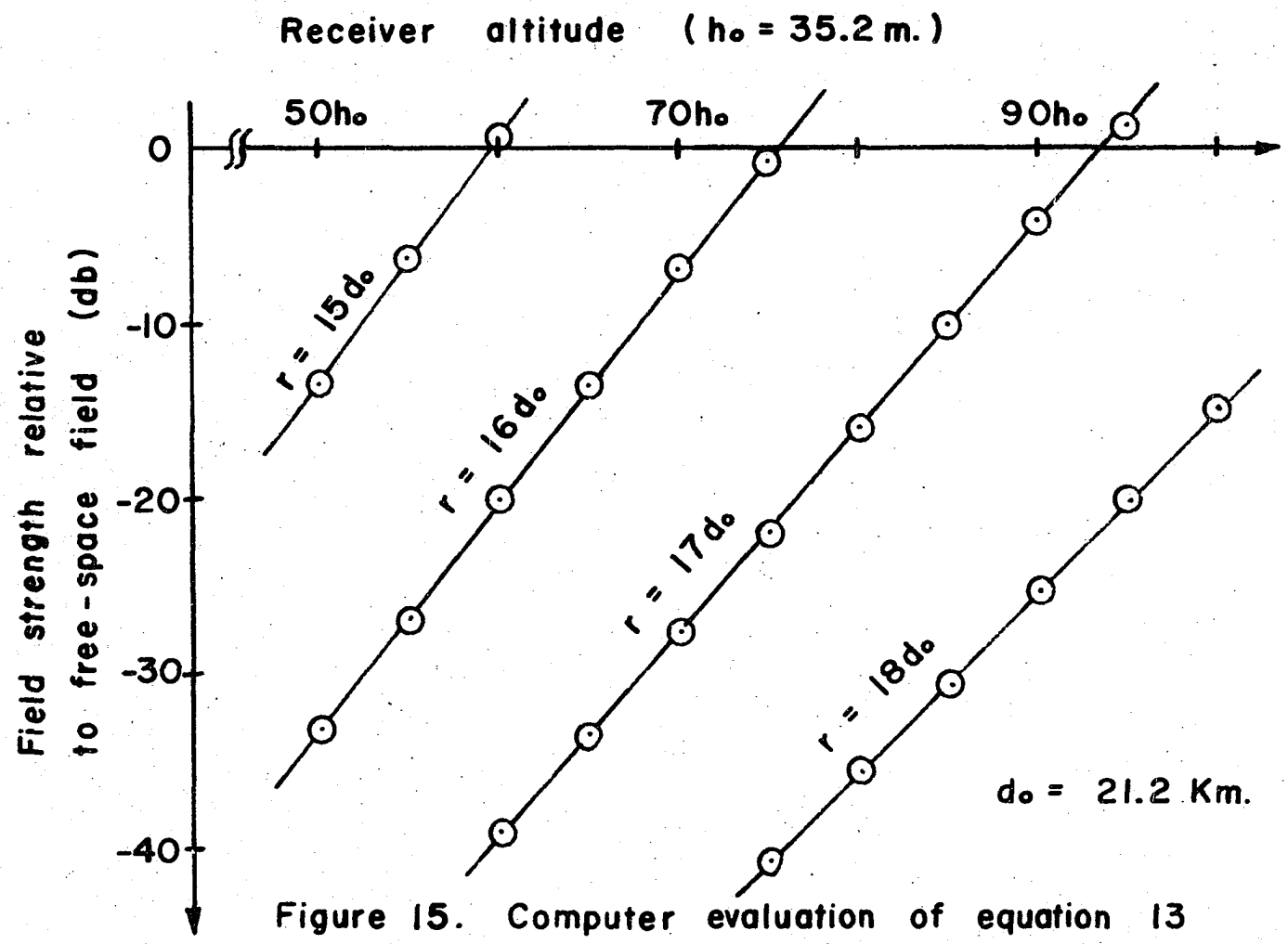

Figure 15. Computer evaluation of equation 13 for five terms (transmitter altitude = 60h_o)

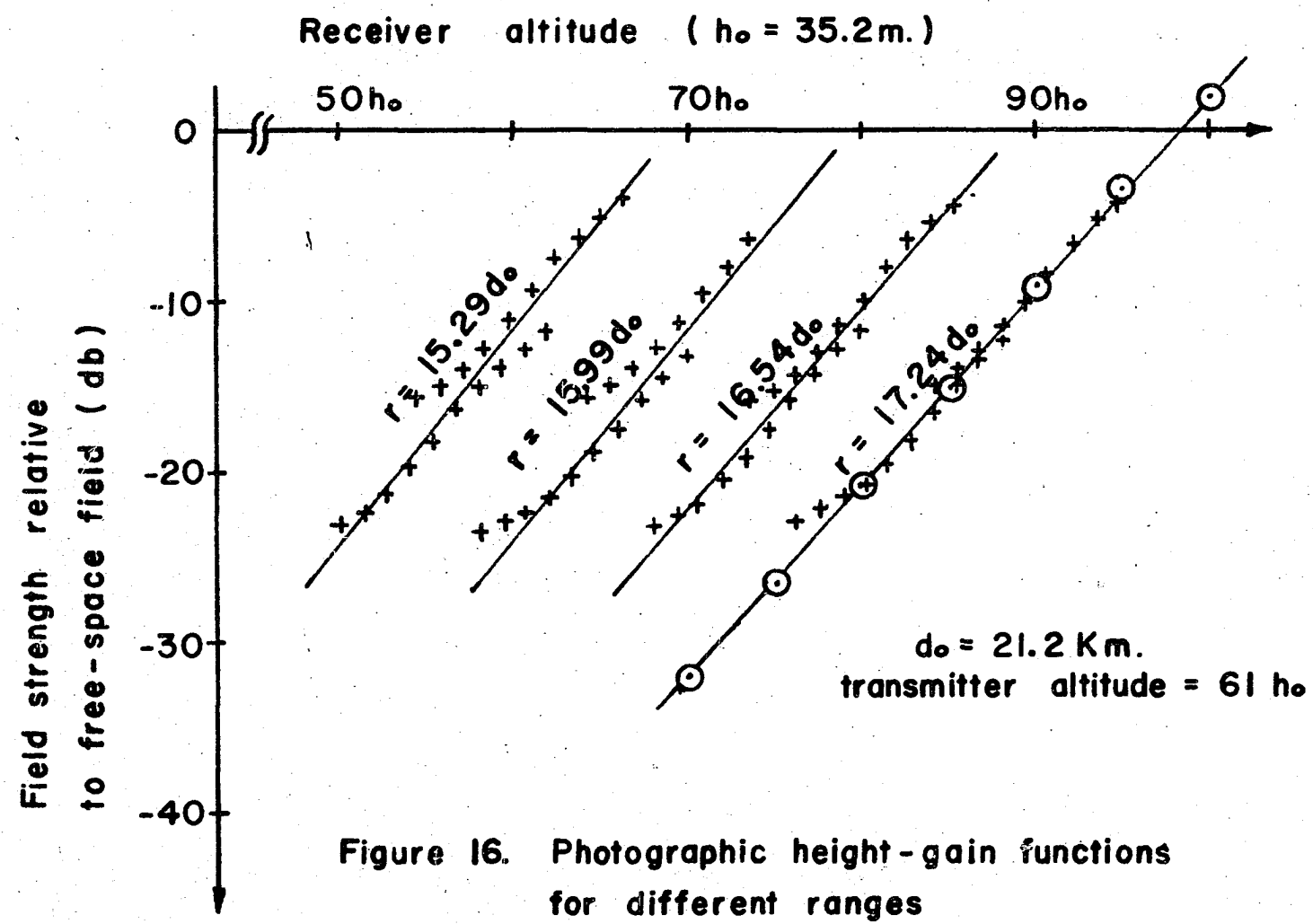

Figure 16. Photographic height-gain functions for different ranges

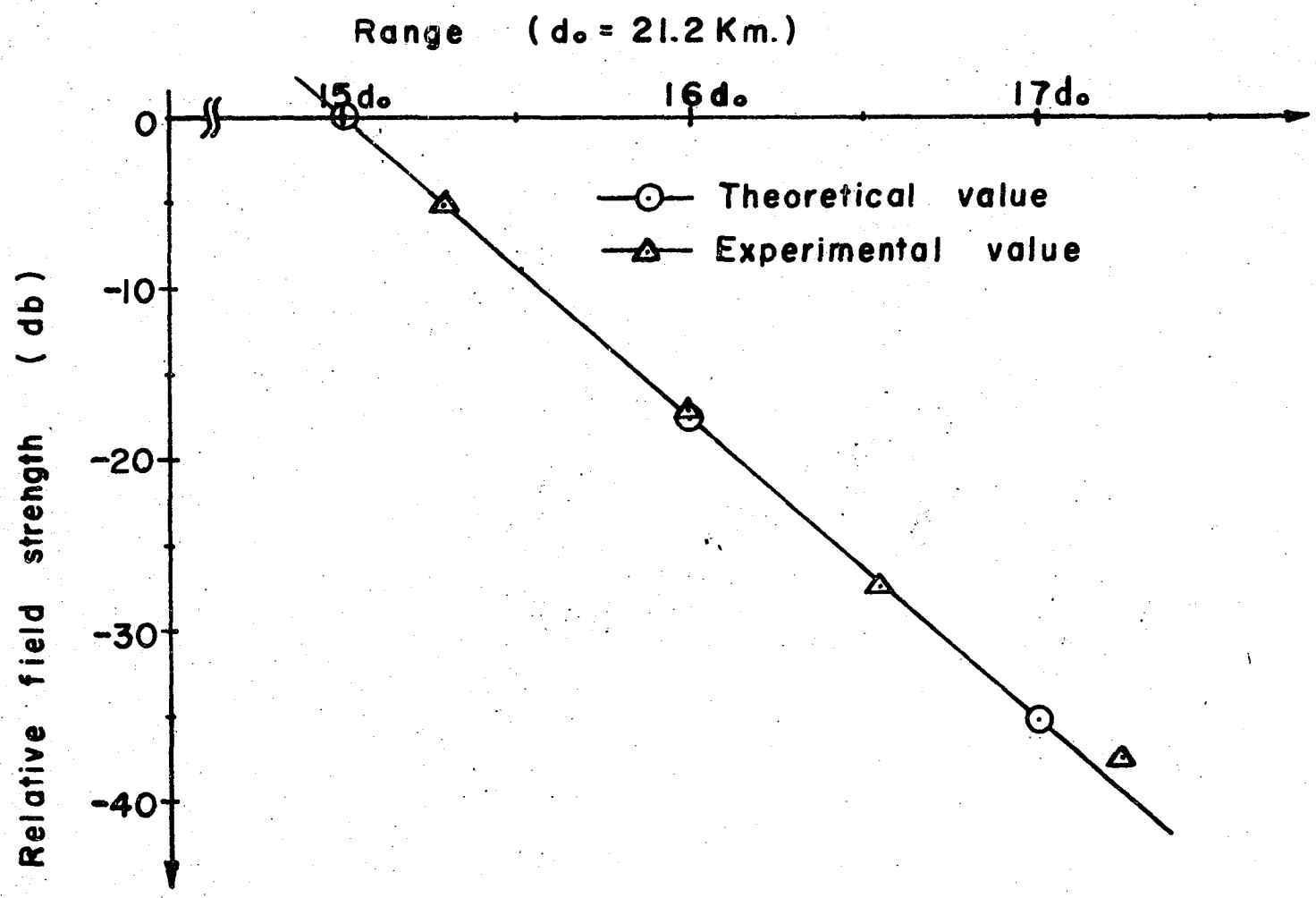

Figure 17. Range attenuation

V. CONCLUSIONS

It has been shown that a laser can be used successfully as a source in scaling atmospheric propagation problems. This permits quantitative measurements of the effects of earth curvature to be obtained experimentally in the laboratory. The use of photographic film has proven to be a convenient and very accurate method for measuring the field distribution. The reproducibility of the results is quite good. Excellent agreement between the diffraction theory of Pryce and measurements has been obtained in the region covered by the measurements. Extensions to include new parameters in the model should prove useful.

Several improvements in the experimental set-up are possible. It may be possible to find a better film-developer combination. Panatomic X is a relatively slow film and a faster film would detect weaker fields with shorter exposures. A good replacement might be Kodak Plus X Pan sheet film. As Panatomic X, it is a fine grain film but rates higher in resolution and acutance. It has a speed almost 2 times greater than Panatomic X. Glass plates would be more convenient to scan, since the microphotometer is constructed to hold them, however, batch processing of plates is more difficult.

It may also be possible to find a developer which will give low saturation gammas for the film used. By processing

to saturation, all adjacency effects would be eliminated. Adjacency effects cause the value of gamma to decrease as one moves into a dense region of the film. The effect appears very much like saturation of the emulsion at the shoulder of the characteristic curve as shown in Figure 10. In the measurements shown in Figure 14, after a region of constant gamma, a decrease in gamma is apparent. This is not saturation of the emulsion since the density is only about 1.2 and much higher densities are required for saturation. It is a decrease in gamma due to adjacency effects. Elimination of the adjacency effects would result in a wider region of constant gamma and thus, a wider latitude. Huntley (16) mentions in his work the availability of special film with very wide dynamic range. This film was found to be, in essence, three separate emulsions of different speeds on one support. It is processed as color film and the results are in terms of color. One must then use a color filter in the microphotometer to scan one or another emulsion. In an experiment where repeated measurements may be made using different film, there does not appear to be any advantage to the use of film of this type.

New lasers are being developed with higher output powers and through their use and the use of more efficient collimating lenses, it would be possible to measure fields

much further beyond the horizon than measured in this experiment. This would permit verification of the theory over wider ranges. Several extensions are suggested. They include measurements of effects of an atmosphere, effects of surface roughness, and changes in field patterns due to mixed path propagation. It is the hope that this study will provide a beginning for future studies involving more conditions as encountered in the actual earth's environment.

VI. LITERATURE CITED

1. Abraham, L. G. and Bradshaw, J. A. Weather and reception level on a troposphere link; annual and short term correlations. National Bureau of Standards Journal of Research. 65D: 155-156. 1961.

2. Bloom, A. L. Properties of laser resonators giving uniphase wave fronts. Spectra Physics (Mountain View, Calif.) Laser Technical Bulletin 2. 1963.

3. Booker, H. G. and Gordon, W. E. A theory of radio scattering in the troposphere. Institute of Radio Engineers Proceedings 38: 401-412. 1950.

4. Budden, K. G. The wave-guide mode theory of wave propagation. Englewood Cliffs, N. J. Prentice-Hall, Inc. 1961.

5. Bullington, K. Propagation of uhf and shf waves beyond the horizon. Institute of Radio Engineers Proceedings 38: 1221-1222. 1950.

6. Bullington, K. Radio propagation variations at vhf and uhf. Institute of Radio Engineers Proceedings 38: 27-32. 1950.

7. Carroll, T. J. Tropospheric propagation well beyond the horizon. Institute of Radio Engineers Transactions on Antennas and Propagation AP-2: 9-27. 1952.

8. Carroll, T. J. and Ring, R. M. Twilight region propagation of short radio waves by modes contained in the normal air. Massachusetts Institute of Technology Lincoln Laboratory Technical Report TR-190. 1958.

9. Domb, C. Tables of functions occurring in the diffraction of electromagnetic waves by the earth. Advances in Physics 2: 96-102. 1953.

10. Edison, A. R. An acoustical modeling experiment for wave propagation in a random medium. Institute of Electrical and Electronics Engineers Transactions on Sonics and Ultrasonics SU-11: 30-33. 1964.

11. Fox, A. G. and Li, T. Resonant modes in a maser interferometer. Bell System Technical Journal 40: 453-488. 1961.

12. Furutsu, K. On the theory of radio wave propagation over inhomogeneous earth. National Bureau of Standards Journal of Research 67D: 39-62. 1963.

13. Gerks, I. H. Introduction to the problem of propagation in a stratified atmosphere over a spherical earth. Unpublished multilithed memorandum. Cedar Rapids, Iowa. Collins Radio Company. 1963.

14. Gerks, I. H. Propagation at 412 megacycles from a high power transmitter. Institute of Radio Engineers Proceedings 39: 1374-1382. 1951.

15. Huntley, W. H. A new approach to antenna scaling. Institute of Electrical and Electronics Engineers Transactions on Antennas and Propagation AP-11: 591-592. 1963.

16. Huntley, W. H. New coherent light diffraction techniques. Institute of Electrical and Electronics Engineers Spectrum 1: 114-122. 1964.

17. Huntley, W. H. The potential of techniques using coherent light diffraction. Stanford Electronics Laboratory System's Techniques Laboratory Technical Report 1963-1. 1963.

18. Jackson, J. D. Classical electrodynamics. New York, N. Y. John Wiley and Sons. 1962.

19. Jenkins, F. A. and White, H. E. Fundamentals of physical optics. New York, N. Y. McGraw-Hill Book Co., Inc. 1937.

20. Johnson, R. W. A normal mode solution to radio wave propagation in a terrestrial environment. Unpublished Ph.D. thesis. Ames, Iowa. Library, Iowa State University of Science and Technology. 1964.

21. Maley, S. W. and King, R. J. Impedance of a monopole antenna with a circular conducting-disk ground system on the surface of a lossy half-space. National Bureau of Standards Journal of Research 65D: 183-188. 1961.

22. Maley, S. W. and Ottesen, H. An experimental study of mixed path ground wave propagations. National Bureau of Standards Journal of Research 68D: 915-918. 1964.

23. Mees, C. E. K. The theory of the photographic process. New York, N. Y. The Macmillan Co. 1954.

24. Megaw, E. C. S. The scattering of electromagnetic waves by atmospheric turbulence. Nature 166: 1100-1104. 1950.

25. Negative making with Kodak black and white sheet films. Rochester, N. Y. Eastman Kodak Corp. 1962.

26. Pekaris, C. L. Accuracy of the earth-flattening approximations in the theory of microwave propagation. Physical Review 70: 518-522. 1946.

27. Post, R. E. The flat-earth approximation to the solution of electromagnetic propagation in a stratified terrestrial atmosphere. Unpublished Ph.D. thesis. Ames, Iowa. Library, Iowa State University of Science and Technology. 1962.

28. Processing chemicals and formulas for black and white photography. Rochester, N. Y. Eastman Kodak Corp. 1963.

29. Pryce, M. H. L. The diffraction of radio waves by the curvature of the earth. Advances in Physics 2: 67-95. 1953.

30. Rayleigh, Lord. The transmission of light through an atmosphere containing small particles in suspension. Philosophical Magazine Ser. 5, 47: 375-384. 1899.

31. Schelleng, J. C., Burrows, C. R. and Ferrell, E. B. Ultra-short-wave propagation. Institute of Radio Engineers Proceedings 21: 427-463. 1933.

32. Silver, S., ed. Microwave antenna theory and design. Massachusetts Institute of Technology Radiation Laboratory Series. Vol. 12. New York, N. Y. McGraw-Hill Book Co., Inc. 1949.

33. Skolnik, M. I. A method of modeling array antennas. Institute of Electrical and Electronics Engineers Transactions on Antennas and Propagation AP-11: 97-98. 1963.

34. Summary of normal mode theory symposium. Institute of Radio Engineers Transactions on Antennas and Propagation AP-4: 90-94. 1956.

35. Tolopko, L. N. Research aims at improved com systems. Electronic News 9, No. 455: 4. 1964.

36. van der Pol, B. and Bremmer, H. The propagation of radio waves over a finitely conducting earth. Philosophical Magazine Ser. 7, 25: 817-834. 1938.

37. Wait, J. R. Radiation from a dipole over a stratified ground. Institute of Radio Engineers Transactions on Antennas and Propagation AP-1: 9-12. 1953.

38. Watson, G. N. The diffraction of electric waves by the earth. Royal Society of London Proceedings Series A, 95: 83-99. 1919.

33. Skolnik, M. I. A method of modeling array antennas. Institute of Electrical and Electronics Engineers Transactions on Antennas and Propagation AP-11: 97-98. 1963.

34. Summary of normal mode theory symposium. Institute of Radio Engineers Transactions on Antennas and Propagation AP-4: 90-94. 1956.

35. Tolopko, L. N. Research aims at improved com systems. Electronic News 9, No. 455: 4. 1964.

36. van der Pol, B. and Bremmer, H. The propagation of radio waves over a finitely conducting earth. Philosophical Magazine Ser. 7, 25: 817-834. 1938.

37. Wait, J. R. Radiation from a dipole over a stratified ground. Institute of Radio Engineers Transactions on Antennas and Propagation AP-1: 9-12. 1953.

38. Watson, G. N. The diffraction of electric waves by the earth. Royal Society of London Proceedings Series A, 95: 83-99. 1919.

VII. ACKNOWLEDGMENTS

The author wishes to express his appreciation to Dr. A. A. Read, his major professor, for his constructive comments and suggestions during the preparation of this thesis and the experimental work preceding it. Special thanks also go to Dr. R. E. Post for his suggestion of the topic, his successful effort to secure financial support, and his continued interest and help.

The author also wishes to express his sincere gratitude to Mr. R. Kniseley of the Atomic Energy Commission Ames Laboratory and Dr. P. Carr of the Iowa State University Physics Department, whose knowledge of the photographic process provided many helpful suggestions; Mr. L. Facto and Mr. R. Van Zee of the Iowa State Photographic Laboratory for their skilled assistance in the photographic development process; Mr. W. Sutherland of the Atomic Energy Commission Ames Laboratory for the use of the microphotometer assigned to his laboratory; Mr. R. Eder of Optics for Industry for his suggestions and assistance in the model construction; and to Mr. R. Anwyl of Eastman Kodak Company for his helpful suggestions and continued interest.

The author also wishes to thank his wife and children for their patience and encouragement which made this thesis possible.